Construction and Characterization of a Fine-Tuned Lytic Phage Display System

by

Jessica Nicastro

A thesis
presented to the University of Waterloo
in fulfilment of the
thesis requirement for the degree of
Master of Science
in
Pharmacy

Waterloo, Ontario, Canada, 2014

AUTHOR’S DECLARATION

I hereby declare that I am the sole author of this thesis. This is a true copy of this thesis, including any required final revisions, as accepted by my examiners. I understand that my thesis may be made electronically available to the public.

ABSTRACT

Bacteriophage (phage) Lambda (λ) has played a key historic role in driving our current understanding of molecular genetics. The lytic nature of this bacterial virus along with the conformation of its wild-type capsid protein (gpD) assembly offer many advantages for the virus for a phage display platform. Protein gpD has been used extensively for fusion polypeptides that can be expressed from plasmids in *Escherichia coli* and persevere, or even increase, solubility.

In this study, the exploitation of gpD for the design of a dual expression system for the display of enhanced green fluorescent protein (eGFP) was developed and characterized. In this system, gpD expression is encoded by mutant λ infecting phage particles, λ*D*am, that can only produce a wild type length gpD allele within specialized strains of *E. coli* that can suppress the mutation. However, the functionality of gpD alleles, produced by passage of λ*D*am through various suppressor strains, varies dramatically in their ability to restore functional packaging to the λ*D*am phage, imparting a first dimension of decorative control.

As a second dimension of decorative control, a *D::eGFP* translational fusion on a multicopy plasmid, encoding gpD::eGFP, complements the *Dam* mutation *in trans* and is regulated by the temperature-labile λ CI[Ts]857 repressor, allowing for the conditional expression of *D::eGFP* by thermoregulation.

In combination, the effective exploitation of these two variables has permitted the effective development of a fine-tuned λ lytic phage display system. Of the suppressor-imparted alleles, gpDQ68S, gpDQ68Y, and gpD_{wt}: the allele with the poorest functionality, gpDQ68S (SupD), in combination with submaximal expression of gpD::eGFP conferred the highest incorporation of the fusion into the λ*Dam* phage capsid in all combinations. Differences in size, fluorescence, and absolute protein decoration between phage preparations was achieved by varying the temperature of the suppressor host carrying the *D::eGFP* fusion plasmid. The effective preparation with these two variables provides a simple means to manage fusion decoration on the surface of phage λ for a variety of fusion partners and applications.

ACKNOWLEDGEMENTS:

I would like to take the opportunity to thank those individuals, who without which this research would not be possible.

I would like to thank my supervisor Dr. Roderick Slavcev. I feel extremely blessed to have had a supervisor that has gone well beyond his duties as a mentor. He has provided support, endless patience, and has given ample opportunities to facilitate my growth as a leader and as a researcher. He has continuously motivated me to do my best by believing in me and my abilities.

I would also like to thank my committee member Dr. Marc Aucoin for his assistance with designing and overtaking the flow portion of the study and his thoughtful feedback on my thesis defense and write-up. I would also like to thank Stanislav Sokolenko for his work with the flow cytometry analysis.

I would like to thank Dr. Michael Beazely for being an excellent committee member, providing consultation regarding my protein work, and asking thought-provoking questions that improved the quality of my defense.

On a personal note, I would like to thank the people who have supported me throughout my graduate studies. I could not have completed this research without the help and support of my lab members: Dr. Nafiseh Nafissi, Farah El-Zarkout, Chi-Hong Sum, Heba Alattaas, Shirley Wong, Katlyn Sheldon, Tranum Kaur, and our undergraduate volunteers and work-

studies. We truly have a wonderful group dynamic. I will cherish our laughs in the office and am pleased to know that I have made some life-long friends.

I would also like to thank my friends from the School of Pharmacy, especially Rabiya Chandani, Samantha Shortall, Anil Maharaj, Wesseem Osman, and Nawaz Ahmed. These are the individuals who gave me a reason to leave my research cave for a bit and celebrate the best moments of this time while also providing support and encouragement during the difficult ones. I am truly grateful I am to have had the opportunity to know each and every one of you.

Last but certainly not least, I would like thank my mother Jacqueline, my father Joseph, my sisters Maggie and Maria, my Nonna Antoinetta, and the rest of the Nicastro-Short clan. You are my foundation and my inspiration.

DEDICATION:

I would like to dedicate this work to my late grandfather Harold Short, my original inspiration into the research of the unknown.

TABLE OF CONTENTS

LIST OF TABLES

LIST OF FIGURES

Table of Abbreviations:

(phage) 21	A temperate lambdoid phage of *E. coli*
a.a.	Amino acid
ADE	Antibody-dependent enhancement, facilitates viral entry into cells
AMP	Ampicillin, a beta-lactam antibiotic
APC	Antigen-presenting cell
BB4	Suppressor *E. coli* strain (*supE supF hsdR*) that is a high efficiency plating natural host for bacteriophage λ and amber mutant derivatives
BPA	Bisphenol A, used as a gpD fusion
cDNA	Complementary DNA, synthesized from an mRNA template
CI	λ repressor gene product, allows phage to reside in lysogenic state
cI	λ *cI* repressor gene
cI[Ts]	Temperature-sensitive alleles of the λ *cI* repressor
cI857	A common temperature-sensitive allele of the λ *cI* repressor
cis	Acting within the same DNA molecule and dominant
CD40	A co-stimulatory protein found on antigen presenting cells and required for their activation
CD51/CD61	The complex formed between the CD51 and CD61 molecules (alpha V and beta 3 integrins) it is also known as the integrin $\alpha_v\beta_3$
CpG	Sequence of bases where cytosine and guanine occur next to each other (CpG is shorthand for cytosine-phosphate-guanine)
Cro	λ (anti-)repressor gene product that acts to turn off early gene transcription during the lytic cycle.
C-Terminal	Carboxy end of an amino acid chain terminated by a free carboxyl group (-COOH)
D	Gene encoding gene product D

D-	Resultant of a lack of complementation of *Dam* with pD
D+	Resultant of the complementation of *Dam* with pD
DLS	Dynamic light scattering, a technique that can be used to determine the size distribution profile of small particles
DNA	Deoxyribonucleic acid
dsDNA	Double stranded DNA
E	Gene encoding gene product E
*Eco*R1	An endonuclease enzyme that is part of the restriction modification system of *E. coli*
eGFP	Gene encoding enhanced green fluorescent protein
EDTA	Ethylenediaminetetraacetic acid, a chelating agent that possesses the ability to sequester divalent metal cations such as Mg^{2+}
EHEC	Enterohaemorrhagic *E. coli*, a bacterium characterized for its ability to cause severe foodborne disease
ELISA	Enzyme-linked immunosorbant assay
EM	Electron microscopy, a technique that uses accelerated electrons as a source of illumination
Env	HIV-1 envelope protein
EOP	Efficiency of plating, the relative viability of phage sample in comparison to a positive control
F1	A filamentous ssDNA bacteriophage
FACS	Fluorescence-activated cell sorter
Fc	Fragment crystallizable region of the tail region of an antibody that interacts with Fc receptors on immune cells
FcγR	Protein receptor found on the surface immune cells, especially important for inducing phagocytosis of opsonized (coated) microbes
Fd	A filamentous ssDNA bacteriophage
Ff	A filamentous ssDNA bacteriophage

FL	Fluorescence, as measured via flow cytometry
GFP	Green fluorescent protein
glnV44	Mutation encoding amber suppressor strain W3101 SupE
gp140	HIV-1 envelope glycoprotein gp160 extracellular domain
gpD	λ gene product D, a major structural protein in the λ phage capsid head
gpDQ68S	Allele conferred from growing λF7 on amber suppressor strain W3101 SupD (*serU132)* which inserts amino acid serine in place of the amber stop codon
gpD_{wt}	Allele conferred from growing λF7 on amber suppressor strain W3101 SupE (*glnV44)* which inserts amino acid glutamine in place of the amber stop codon
gpDQ68Y	Allele conferred from growing λF7 on amber suppressor strain W3101 SupF *(tyrT5888)* which inserts amino acid tyrosine in place of the amber stop codon
gpE	λ gene product E, a major structural protein in the λ phage capsid
gpV	λ gene product V, the major tail protein for λ phage
HBsAG	Surface antigen of the Hepatitis B virus
HCV	Hepatitis C virus
HIV-1	HIV type 1, the virus responsible for AIDS
Hoc	Major coat protein of T4 phage, present at ~155 copies
Hpa1	An endonuclease enzyme that is part of the restriction modification system of *E. coli*
HUS	Haemolytic-uraemic syndrome, a disease commonly preceded by the infection with *E. coli* O157:H7
IgG	Immunoglobulin G antibody isotype
Imm	Immunity, in phage biology this is the
Ind-	Mutation precluding cleavage of a temperature-sensitive repressor such as LexA[Ts] or CI[Ts]857

IPTG	Isopropyl β-D-1-thiogalactopyranoside, a molecular biology reagent.
Kpn1	An endonuclease enzyme that is part of the restriction modification system of *E. coli*
Lambda (λ)	*E. coli* temperate, siphoviridae family bacteriophage
λ*D*am	λ phage that contains an amber mutation within the gene for protein gpD and thus can only produce wild-type length gpD alleles within specialized strains of *E. coli*
λF7	Synonymous with *λDam15imm21cIts* that possesses a defective (suppressible) *D* gene and the immunity region (*imm*) of phage 21
λKM4	λ phage vector that can accept inserts of up to 3 kb in length as *D::X* fusions without disturbing λ packaging
λKM8	λ *D::X* fusion (C-terminal) phage vector derived from λKM4
λKM10	λ *D::X* fusion (N-terminal) phage vector derived from λKM4
LB	Luria Bertani broth, a widely used rich culture medium, for growth of bacteria and phage
M13	A filamentous ssDNA bacteriophage
MCS	Multiple cloning site, a short segment of DNA within a plasmid containing numerous restriction sites that are typically used during molecular cloning or subcloning procedures
N15	An *E. coli* bacteriophage similar in structure, but not genetic composition, to bacteriophage λ
Nco1	An endonuclease enzyme that is part of the restriction modification system of *E. coli*
N-Terminal	Amino end of a polypeptide chain, terminated by a free amine group ($-NH_3$)
O157:H7	Serotype of an enterohemorrhagic strain of *E. coli* (EHEC) encoding the Shiga toxin
O_L	Leftward transcription operator of bacteriophage λ
O_R	Rightward transcription operator of bacteriophage λ

PBS	Phosphate buffered saline
PCR	Polymerase chain reaction
pD	plasmid-borne D, resultant of the complementation of *Dam15* from a plasmid
PEG	Polyethylene glycol
PFU	Plaque forming unit—single immobilized phage that grows to form a plaque on an agar cell lawn. A means of calculating lysate titer
pIII	Minor coat protein of M13 phage, present in ~5-6 copies and commonly used as a fusion protein for phage display
PMT	Photomultiplier tube, member of the class of vacuum tubes used in this study for flow cytometry
pVI	Minor coat protein of M13 phage, present in ~5-6 copies
pVII	Minor coat protein of M13 phage, present in ~5-6 copies
pVIII	Major coat protein of M13 phage, present in ~2700 copies and commonly used as a fusion protein for phage display
pIX	Minor coat protein of M13 phage, present in ~5-6 copies
P_L	Rightward strong transcription promoter of bacteriophage λ
PP01	Virulent phage specific to *E. coli* O157:H7
P_R	Leftward strong transcription promoter of bacteriophage λ
RecA	Prokaryotic protein essential for the repair, maintenance and homologous recombination of DNA
recA	Gene encoding the RecA protein (above)
RSV	Respiratory Syncytial Virus, the major cause of respiratory disease in young children
SDS	Sodium dodecyl sulfate
SDS-PAGE	Sodium dodecyl sulfate polyacrylamide gel electrophoresis, a common method to separate proteins according to their size

scFv	Single-chain variable fragment, a fusion protein of the variable region of immunoglobulins. This fragment has been commonly used as a random display peptide in phage display to isolate new mAbs
serU132	Mutation encoding amber suppressor strain W3101 SupD
SOC	Major coat protein of T4 phage, present in ~870 copies
SPA	sequential peptide affinity tag
SSC	Side-scatter, as measured via flow cytometry
ssDNA	Single stranded DNA
Sup-/*sup*-	A wild type *E. coli* strain that does not confer any suppressor activity
Sup^+/sup^+	A mutant *E. coli* strain that confers suppressor activity to conditional mutations
SupD/*supD*	A tRNA mutation in *E. coli* that suppresses the amber stop codon conditional mutation (UAG) by reading this codon and inserting instead a serine amino acid
SupE/*supE*	A tRNA mutation of *E. coli* that suppresses the amber stop codon, inserting instead a glutamine amino acid at this codon
SupF/*supF*	A tRNA mutation of *E. coli* that suppresses the amber stop codon by inserting instead a tyrosine amino acid at this codon
ssDNA	Single-stranded DNA
T4	Member of the lytic T-even myoviridae bacteriophage of *E. coli* that is only capable of undergoing a lytic lifecycle
T7	Member of the type T podoviridae bacteriophage family that infects *E. coli*. This phage is only capable of undergoing a lytic lifecycle
TAT	Gene product of the *tat* gene, the "Trans-activator of Transcription", from HIV-1 which acts as a regulatory protein by dramatically enhancing endocytosis and the efficiency of viral transcription
T_h1	T_h1 helper cells, initiate the host immunity effectors against intracellular bacteria and protozoa
trans	The action/repression/substitution of a gene in one chromosome on a gene product on another chromosome

tRNA	Transfer RNA, physical link between the nucleotide sequence of nucleic acids (DNA/RNA) and the amino acid sequence of proteins
Ts	Temperature-sensitive
tyrT5888	Mutation encoding amber suppressor strain W3101 SupF
UAG	Amber stop codon
UAA	Ochre stop codon
UV	Ultraviolet, a type of electromagnetic radiation that can negatively affect the life of a bacterial organism
V	Gene encoding gene product V
W3101	*E. coli* strain (F-, *galT22, λ-, IN(rrnD-rrnE)1, rph-1*) that is a high efficiency plating natural host for bacteriophage λ

Chapter 1: Literature Review of Selected Materials

1 Literature Review of Selected Materials

This review is adapted from a previously published article in the Journal of Applied Microbiology and Biotechnology (Nicastro et al. 2014).

1.1 Introduction to Phage Display

Bacteriophage (phage) are bacterial parasites that, like their animal virus counterparts, exist in a variety of morphologies and with diverse genetic architectures. Most phage are limited in their host range, normally infecting only a single species of bacteria, and often only a subset of that species, adsorbing to specific receptors on bacterial cells that define their host range. Lytic phage such as T4 and T7 enter immediately into a state of reproduction upon infection, lysing the cell. In contrast, temperate phage such as bacteriophage Lambda (λ) "choose" between vegetative growth and a quiescent state where the phage genome is stably harbored in the host cell in a state called lysogeny. Filamentous phage, such as M13 (Figure 2) and Ff do not lyse the cell in any state but rather convert the cell into a phage-producing factory, thereby compromising the host's growth (Gulig et al. 2008).

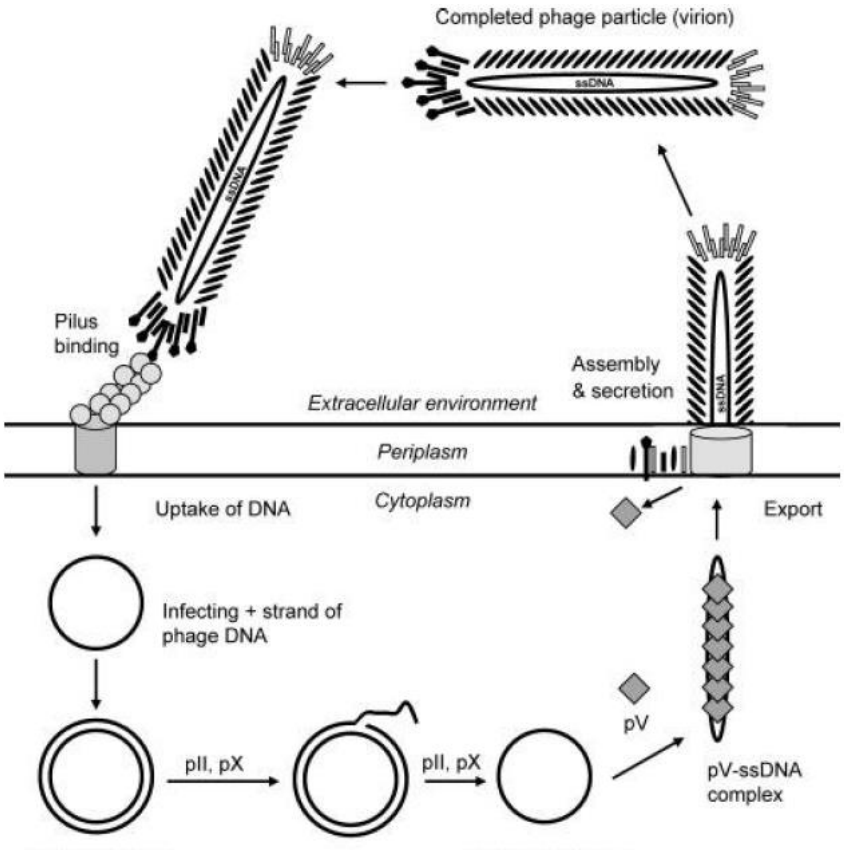

Figure 2: The M13 life-cycle. Phage coat proteins are assembled onto the inner cell membrane before ssDNA is packaged into the capsid and the phage are released from the cell (Kehoe & Kay 2005).

Bacteriophage display, or phage display (Figure 3), was first developed by George Smith in 1985 and can be defined as the process by which a heterologous protein or peptide is expressed as an exterior fusion through the genetic fusion to a coat protein gene of the bacterial virus (phage) particle (Lindqvist 2005). This revolutionary technique, which is one of the largest innovations involving phage since their discovery in the early 1900's (d'Herelle & Smith 1926, Duckworth 1976), is based on the genetic fusion, where the outcome of this

genotypic manipulation (Kaiser 1966) will produce a phenotypic outcome (Jestin 2008). The most well-known phage display methods are based on the usage of phage M13 and the related filamentous phage of *Escherichia coli.* Although filamentous phage are not the focus of this review, the principles of their early use govern phage display advancements. The most extensively used phage are derived from the *E. coli* Ff (filamentous) class, where the most commonly explored species include M13 (Figure 2**)**, fd and f1. The basic structure of these phage consist of a circular single-stranded (ss) DNA genome that is encapsulated by a long tube comprised of thousands of copies of a single major coat protein and four additional minor capsid proteins at the tips. M13 has been especially useful for phage display as its genome is bound only by the major coat protein (as opposed to filling a phage head structure). Therefore, there is not a strict limit on the size of packaged DNA permitting for more opportunities for manipulation. Smith (1985) was the first to successfully demonstrate a phage capsid fusion by inserting an external gene into the phage genome of fd. This construct demonstrated the efficient display of *Eco*RI endonuclease gene product on the fd minor coat protein pIII (Smith 1985, Smith & Huggins 1982). Based on this initial work, lytic phage, including phage T4 and T7, and temperate phage λ would eventually be successfully exploited as fusion vectors as well (Garufi et al. 2005, Kalniņa et al. 2008).

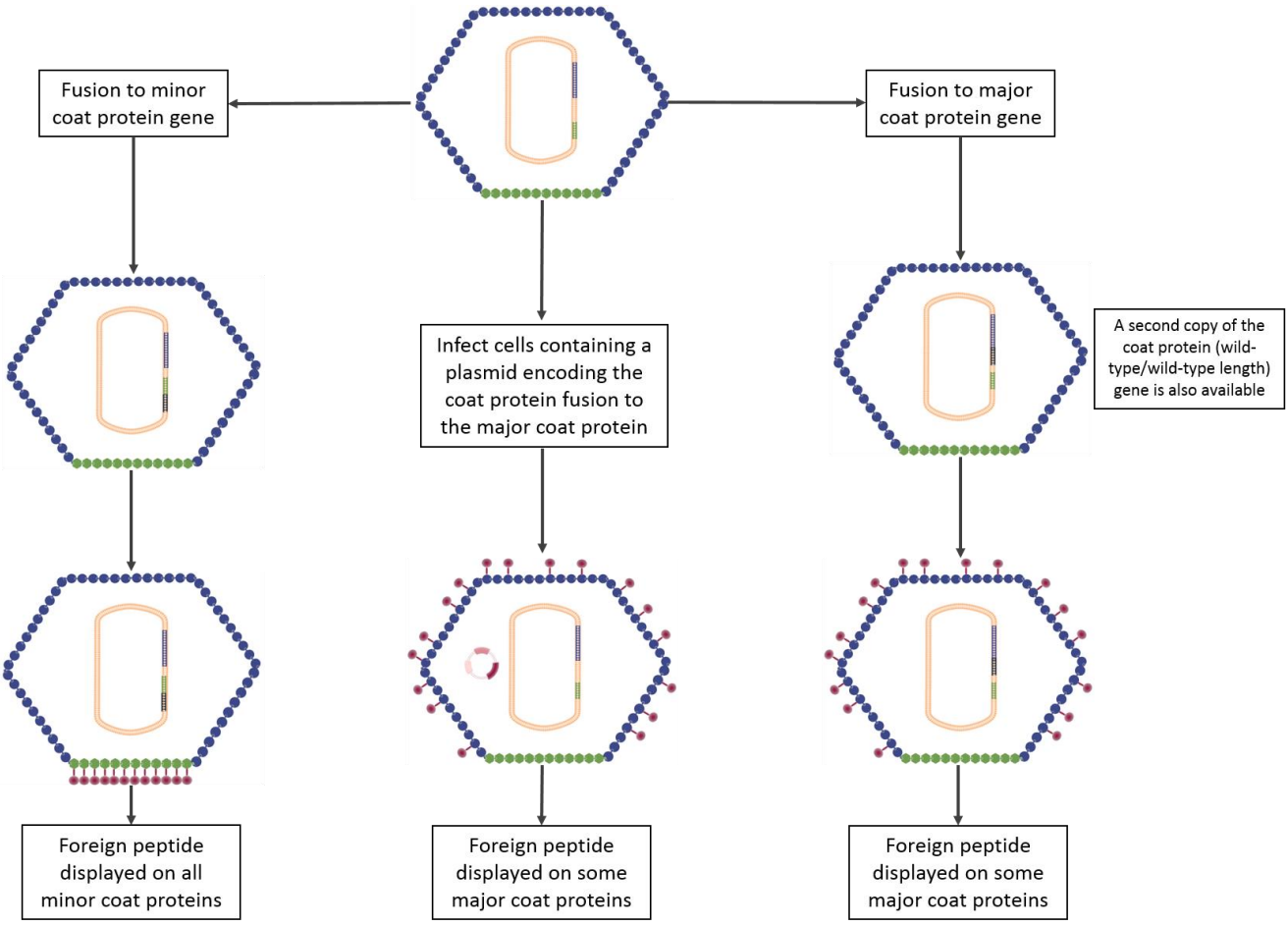

Figure 3: Schematic for phage display. Foreign peptides can generally be displayed on more than one peptide and in varying amounts. The amount of peptides that a phage can tolerate will generally depend on the size of the fusion, where smaller peptides can be tolerated in higher amounts. Fusions may also occur concurrently on minor and major coat proteins, as well as simultaneously on both the N-and C-terminals of the same coat protein.

1.2 Lytic vs. Filamentous Phage Display

The use of filamentous phage in display technology possesses major limitations that can be overcome with lytic phage display systems. First, a tolerated fusion must have the ability to translocate across the plasma membrane and as such, many hydrophilic cytoplasmic proteins cannot be extruded as fusion proteins in filamentous phage, where phage assembly occurs onto the inner cell membrane (Figure 2). Second, filamentous phage are severely constrained by the size of fusions possible (Garufi et al. 2005, Mikawa et al. 1996, Sternberg & Hoess 1995). Third, filamentous phage are dependent on the viability of the host and thus, cannot effectively display peptides/proteins that are toxic to the cell (Garufi et al. 2005). Due to the lytic nature of double-stranded (ds) DNA bacteriophage, the fusion of toxic proteins is no longer a concern in temperate or lytic phage as the phage protein development is repressed in the phage lysogenic state (temperate phage only) and occurs just prior to cell lysis (Garufi et al. 2005).

A few lytic phage candidates have been identified for phage display such as λ, T4 and T7. The C-terminal of T4 minor capsid proteins Hoc and Soc tolerate fusions for lytic phage display (Efimov et al. 1995, Ren et al. 1996). Phage T7 has been employed as a display platform for various GFP-based cytoplasmic proteins that showed poor expression (fluorescence) with more traditional filamentous display vectors (Dai et al. 2008). Santini *et al.* (1998) developed the first chimeric phage system in which C-terminal fusions were made to the λ major capsid protein gene product D or gpD. Recombinant phage were decorated with both wild-type gpD and proteins from a hepatitis C virus (HCV) cDNA expression library. These recombinant phage were compared to two other libraries (N-terminal fusions

to the pIII and pVIII capsid proteins of M13) using the cDNA expression library. In order to avoid overpopulating the λ phage with gpD fusions, and improve the phage stability, they expressed a second *D* allele possessing an amber mutation within the gene for gpD. This addition to the phage display process allowed for the formation of chimeric phage (Santini et al. 1998). Comparing the filamentous phage proteins, pVIII's display was more efficient than pIII, and when pVIII was compared to gpD display and selection of protein fragments of limited size, the two libraries showed comparable efficiencies. However, when larger protein fragments were tested, gpD outperformed pVIII. This result was attributed to the absence of the requirement of λ to secrete the fusion protein. So unlike filamentous pIII/VIII, larger recombinant proteins can fold properly without interfering with phage assembly while displaying higher densities (Santini et al. 1998).

Gupta *et al.* (2003) later designed a λ phage display library that expressed fusions on the C-terminal of gpD. This library was compared to one created by fusing to an M13 phage (N-terminal fusions made utilizing major coat protein PVIII and minor coat protein PIII) where there was no degradation of displayed products. This λ display system provided a 100-fold higher display for all fragments compared to filamentous phage. The λ system generally displayed proteins of different sizes, where the number of fusions/phage particle was 2-3 orders of magnitude greater than that for M13. When the high-density display was applied to epitope mapping, the λ system consistently outperformed M13 with a higher ELISA reactivity shown.

1.3 Bacteriophage λ Phage Display

Bacteriophage λ is one of the most well-studied model temperate bacteriophage to date. Much of what we know about viral and bacterial genetics is owed to previous work in λ phage genetics and regulation. When fully formed, bacteriophage λ has a linear dsDNA genome harboured within an icosahedral capsid, and a flexible, non-contractile tail (Ling et al. 2011, Roberts & Devoret 1983). A great deal of work has been done investigating the genetic switch between lytic and lysogenic states (Ptashne 2004) and the phage's assembly (Roberts & Devoret 1983).

The icosahedral-shaped bacteriophage λ capsid is approximately 60 nm in diameter with a shell thickness of about 4 nm and accommodates the λ genome of 48.5 kb (Hohn & Katsura 1977, Witkiewiczl & Schweiger 1982). Phage λ assembles its head in two steps: prohead assembly followed by DNA packaging. Casjens and Hendrix (1974) identified and described that gene product E (gpE) and gene product D (gpD), comprise the λ icosahedral capsid (Georgopoulos et al. 1983). The λ prohead shell is composed mainly of gpE in approximately 415 copies. DNA packaging requires a conformational change to the prohead via the addition gpD to the prohead, which increases the head volume and stability (Georgopoulos et al. 1983, Yang et al. 2000). Gene product D is present in 405-420 trimer-clustered molecules (Figure 4) and although it is not required for prophage head assembly, it is essential for the packaging of a full-length genome (Beghetto & Gargano 2011). In contrast, gpD deficient viruses can package up to 82% of the wild-type genome (Dokland,T., Murialdo 1993) but need to be stabilized by magnesium ions, and are extremely sensitive to the divalent cation chelator, EDTA (Sternberg et al. 1979, Yang et al. 2000). It has also been suggested that

gpD acts by physically blocking the DNA from leaking through the shell (Dokland,T., Murialdo 1993). Like eukaryotic chromosomal proteins, the gpD proteins are able to cross-react immunologically with eukaryotic histones, which may pertain to gpD's function in the stabilization and compaction of phage DNA (Wendt & Feiss 2004).

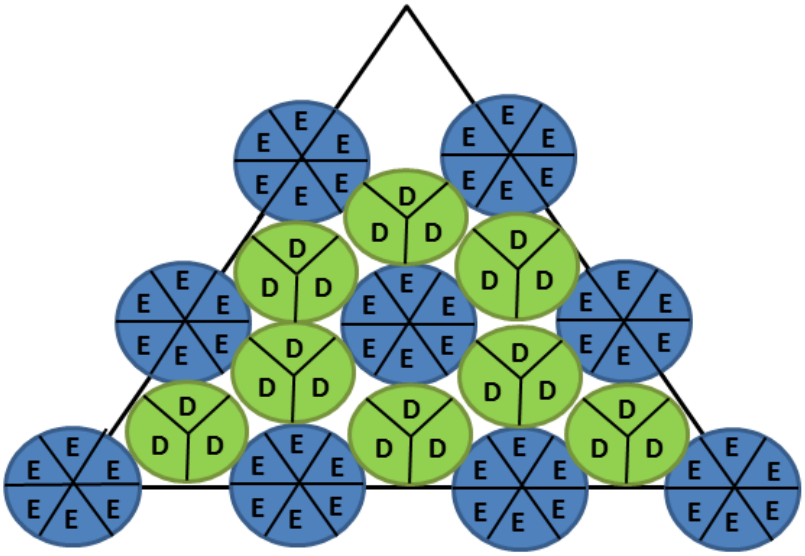

Figure 4: One face of bacteriophageλ. The illustration depicts one of the 20 faces of the bacteriophage λ capsid head. Protein gpD (the decoration protein labeled "D") is incorporated in homotrimers at 405-420 molecules per capsid, and protein gpE (the other major capsid protein labeled "E") is incorporated, at same number, into homohexamers.

1.3.1 Protein gpD as the Lambda Fusion Protein:

Initial λ phage display fusions were fused onto gpV, the major tail protein, present in 192 copies (Dunn 1995) per phage particle. Maruyama et al. (1994) successfully displayed fusion proteins β-galactosidase and BPA to the C-terminal domain of gpV. They did however, discuss limitations to gpV fusions such as the very low fusion expression of less than one fusion/phage particle (Maruyama et al. 1994, Mikawa et al. 1996). It has been suggested that

the fusion proteins may interfere with the tail assembly, imparting the low yield (Maruyama et al. 1994). They also demonstrated conditional fusions through the use of an amber stop codon between the gpV protein at the C-terminal and the gene encoding the fusion enabled functional tail formation (Maruyama et al. 1994), where the display of shorter peptides has since been reported to be well tolerated in all 192 copies (Dunn 1995, Katsura 1983, Zanghi et al. 2007). Phage display fusions on gpD confer a high decoration capacity per phage particle (up to 420) in comparison to the gpV tail protein (~1) (Maruyama et al. 1994, Mikawa et al. 1996) and are conditionally required for phage head assembly compared to gpE, which is absolutely required (Mikawa et al. 1996, Sternberg & Hoess 1995).

Cryo-electron microscopy and image processing of gpD have shown that the major capsid protein assembles in homotrimers that are incorporated as prominent protrusions on the surface of the phage capsid, making them more accessible for binding to external target molecules (Figure 5) (Dokland, Murialdo 1993; Sternberg & Hoess 1995). The use of gpD to express peptides on the λ capsid is ideal since both the N- and C-termini protrude outward, exposing them to tolerate the addition of fused peptides (Mikawa et al. 1996, Witkiewiczl & Schweiger 1982)

.

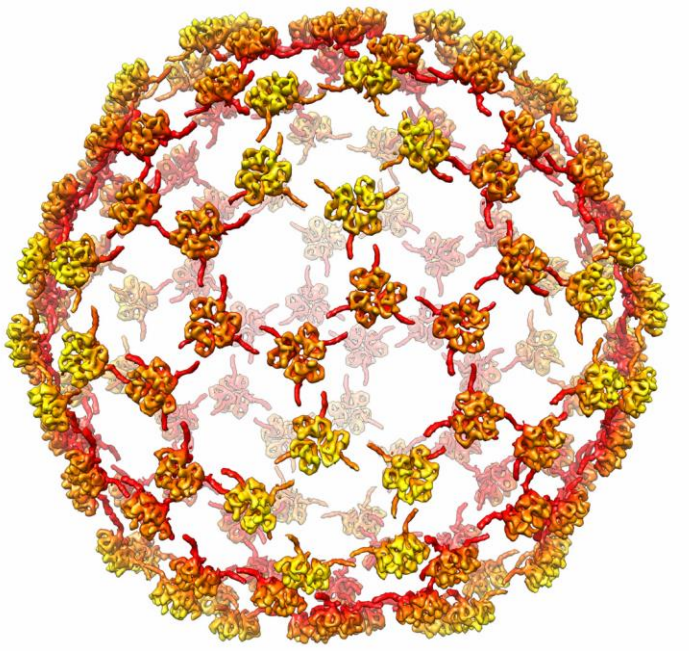

Figure 5: Protein gpD trimers bound to the icosahedral surface of phage λ. The overall network of interactions shows the pattern of gpD. The protein is incorporated at approximately 405-420 copies on the phage λ head and can be seen as strongly protruding thimble-shaped trivalent spikes (Lander et al. 2008).

1.3.2 Amino vs. Carboxy Fusions to gpD

As previously mentioned, the λ gpD protein is tolerant of various protein and peptide fusions to the N- and C-termini (Figure 6) of the major capsid component, providing great flexibility to this lytic phage display system. Pavoni *et al.* (2004) constructed a tumor cDNA display library employing the N-terminal for fusions to gpD in order to prevent the selection of out-of-frame fusions. As such, the recombinant phage can be decorated solely with gpD fusions (Minenkova et al. 2003, Pavoni et al. 2004). Both the use of an N-terminal fusion and engineered phage allow for simpler assembly of chimeric phage, but the use of enhanced green fluorescent protein (eGFP) as an N-terminal fusion partner does not allow for proper

folding of eGFP, compromising its fluorescence in the fusion (Pavoni et al. 2004). Zucconi *et al.* (2001) determined that the number of tolerable fusion proteins displayed on the capsid surface is dependent on the length of the display protein. Furthermore, the group also reported that high incorporation rates is achieved by fusion to either the N- or the C-terminus. These groups provided important initial insight into the ability of gpD fusions to retain function and thus, for phage to assemble properly and form viable phage particles (Minenkova et al. 2003, Zucconi et al. 2001).

Yang et al. (2000) used cryo-electron microscopy to show that the N-terminus of gpD is conditionally disordered when unbound and may interact with gpE. Any fusions to it requires the interaction of the N-terminal fusion linker with gpE to display the fusions on the outside of the fusion proteins. This claim is supported by a study by Lander *et al.* (2008) where a cryo-electron microscopy reconstruction of the λ capsid head was developed and showed that the first 14 residues in gpD N-terminus interact with a strand of an E-loop in gpE and together form a stable β-sheet. This combination allows for the stabilization of the phage head.

Vaccaro *et al.* (2006) fused a functional scFv antibody to the N- and C-termini of gpD and found that the N-terminal fusions showed a relatively low recombinant protein loading in comparison to the C-terminal fusions (50% compared to 88%). The C-terminal fusions also presented unusually small plaques, which suggested that the large scFv protein was compromising phage assembly. They also performed phage stability assays *via* immunoscreening, and observed that while N-terminal phage produced expected results, one to five percent of plaques generated by C-terminal fusions were larger in size and negative

for the assay. These plaques were later found to be mutants possessing point mutations caused either by frame-shift or premature stop signal point mutations within the scFv gene, suggesting a powerful selection against the inefficient display of the antibody as a C-terminal fusion and the inhibitory effect on the assembly of viable phage (Vaccaro et al. 2006).

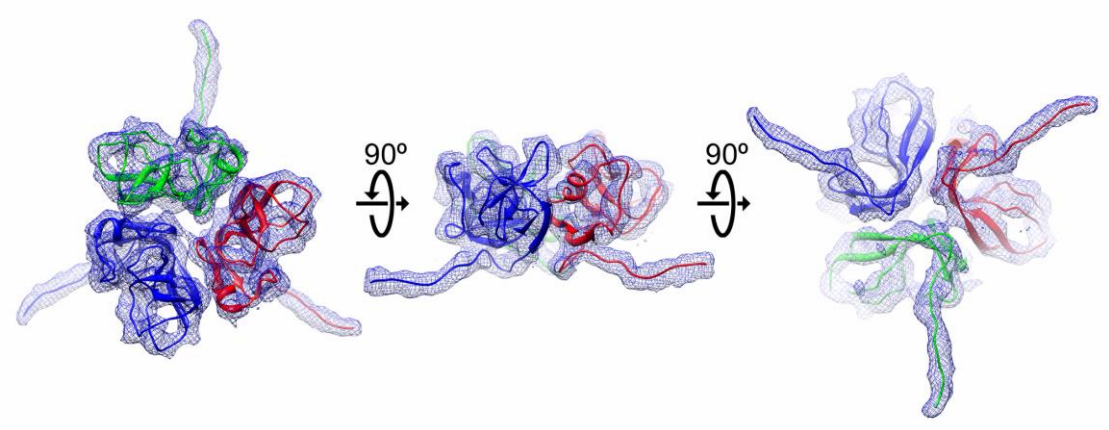

Figure 6: Isolated density pertaining to gpD. The gpD protein is depicted from the top, side and bottom, respectively (left to right) from a crystallized fit into a reconstructed EM structure density. The N-termini of the gpD homotrimer can be seen extending away from the main body. The N-terminus requires the mature capsid substrate for stabilization (Lander et al. 2008).

1.4 Genetic Control Systems

1.4.1 Amber suppression:

Amber suppression is a form of conditional suppression of nonsense codon mutations. Theoretically, a second host site (suppressor) mutation permits a read through of the amber stop codon and insertion of an amino acid (a.a.) in lieu of premature termination. The largest class of nonsense suppression is mediated through tRNA genes where a mutant allele coding for a tRNA of the *E. coli* host (Figure 7) has a modified complementary anticodon for the stop codon which inserts an a.a. in place of the stop codon. This functions to suppress (or prevent) termination (Taira et al. 2006). Amber suppression is specific to the amber (UAG) stop codon (Benzer & Champe 2013, Inokuchi et al. 1979). Other classes of nonsense suppressors include ochre and opal suppressors that recognize UAA and UGA stop codons, respectively, in accordance with Weigle Rules, where both G=U and A=U base pairing can occur (Eggertsson & Söll 1988). Suppressor tRNA is in competition with translation termination factors; therefore the suppression efficiency will be leaky and typically less than 100% (Normanly et al. 1986).

Two translational outcomes occur in suppressor strains: i) non-functional protein truncations; and ii) full-length species conferring partial to complete function. Restoration of the wild-type pristine protein sequence, or a protein sequence that is identical to the original, is preferable to most closely mimic the properties of the original protein (Normanly et al. 1986).

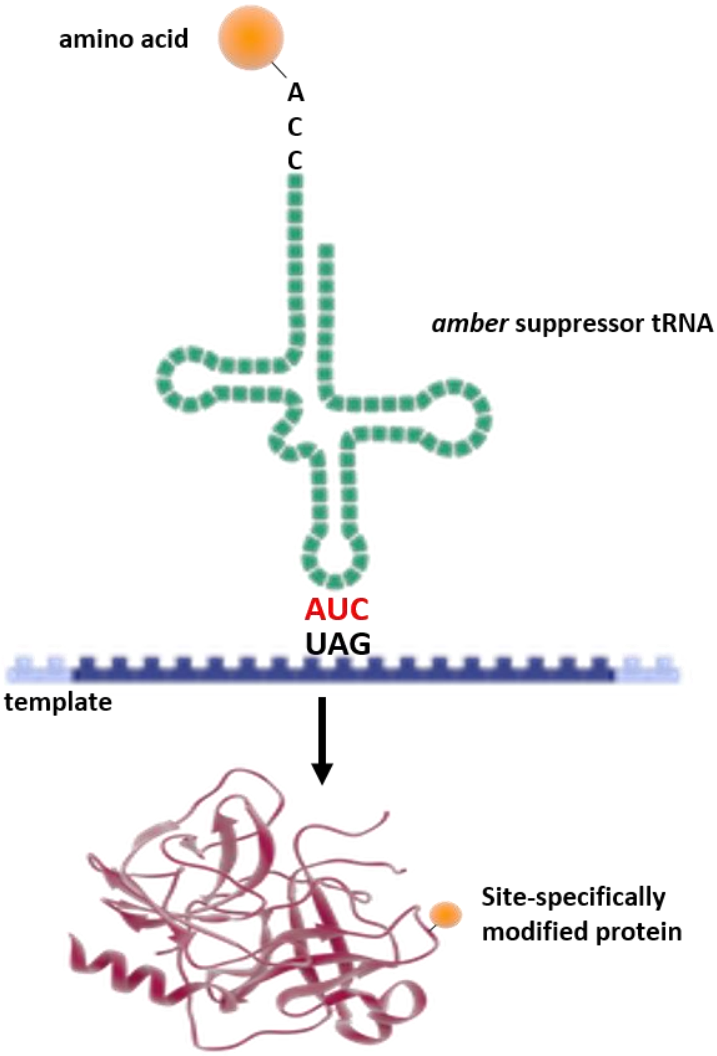

Figure 7: Amber suppression of the λ *Dam15* allele. Amber suppressor strains of *E. coli* possess a mutation that alters tRNA activity, which pairs a charged mutant tRNA with the amber mutation (UAG) and inserts an a.a. in the place of the stop codon. This results in the full translation of *a* wild-type length allele of gpD.

1.4.2 Temperature-conditional λ CI[Ts]857 Repression

Lieb (1966) first characterized the λ CI[Ts]857 temperature-labile repressor and discovered that it was the dissociation of this repressor complex that allowed downstream transcription to proceed from the λ rightward (P_R) and leftward (P_L) strong promoters (Lieb 1966, Szybalski et al. 1969). It is the controllable nature of this repressor associated with expression from a strong promoter that made temperature-sensitive *cI*[Ts] alleles attractive for use in cloning vectors to regulate expression of the gene of interest. In these cases, a single copy of the *cI*[Ts] gene produces enough repressor to effectively inhibit the P_L or P_R promoters on single or multicopy replicons (Bernard et al. 1979, Lukacik et al. 2012, Remaut et al. 1981). Under this repressor-regulated promoter's control, a downstream gene is expressed at increasing levels as temperature increases due to the temperature lability of the CI857 allele. Thermal sensitivity may not be as tightly regulated as chemical induction approaches, but is less likely to be genotoxic, and provides controllable expression attributes that are very favourable. The most common CI857 allele is also "Ind-" that renders the repressor resistant to RecA-catalyzed autocleavage, and thus insensitive to other mutagenic inducers such as UV lending further control over expression (Mott et al. 1985, Ren et al. 1996). The CI857 allele denatures completely at 40-42°C, conferring maximal expression of the gene of interest (Hayes & Hayes 1986). Conversely, temperatures as low as 29°C may be required to fully repress transcription from P_L via the CI857 allele, and highest protein yields can be obtained following induction at 36°C. The temperature efficiency depends on the protein being expressed and the host cell; the expression of many heterologous proteins innately affect bacterial cell growth and survival (Guzmán et al. 1994, Jechlinger et al. 1999,

Lowman & Bina 1990, Villaverde et al. 1993). Strategies to avoid protein expression toxicity include: i) suppression of basal expression from leaky inducible promoters; ii) suppression of read-through transcription from cryptic promoters; iii) tight control of plasmid copy numbers; iv) protein production as inactive (but reversible) forms; and v) the creation of special expression vectors and modified *E. coli* strains (Saïda et al. 2006). The CI857 repressor activity is not limited to *E. coli*; it has also been effective in gram-positive strains such as *Bacillus subtilis,* where downstream expression efficiencies were found to be similar to those reported in *E. coli* with only minor codon bias modifications required (Breitling et al. 1990).

1.5 Controllable Phage Display Systems

Since the development of significant applications derived from the original work on lytic display, control of fusion copy number has been generally underdeveloped. The number of tolerable fusions per phage particle is thought to depend on the size of the fused fragment. Smaller fusion fragments are expected to be tolerated in greater numbers in comparison to their larger counterparts (Gupta et al. 2003). When comparing strategies for the development of a vaccine versus a vector for gene delivery or fusion of a peptide versus a large multimeric protein, many different approaches must be applied due to the differentiation in fusion number. In addition, various factors must be taken into consideration for various downstream applications, including but not limited to: i) the occurrence of over-stimulating a signal due to high affinity or high avidity interactions; ii) the possibility of cross-reactivity and steric hindrance impeding protein function; and iii) ligand access. The control over fusion

decoration is of paramount importance particularly toward the development of phage therapeutics (Figure 8).

Mikawa *et al.* (1996) were first to employ amber suppression to regulate gpD. Although the approach was qualitative and based on relative display, more modern approaches were used to generate gpD fusions *in vivo.* These systems were able to generate libraries and purify functional fusions, increase the size and density of capsid fusions, and recently tackle the issue of copy control (Lankes et al. 2007, Mikawa et al. 1996, Nicastro et al. 2013, Sokolenko et al. 2012). Two unique vector features used in these initial constructs included a peptide linker and the conditional fusions via amber suppression strategies that permitted the fusion of multimeric proteins. There was only a slight difference in expression when suppression was used as a crude control mechanism for capsid fusion expression by employing various allogeneic *E. coli* suppressor strains SupE, SupF, SupD, Sup^{-}, coding for glutamine, tyrosine, serine or no residue (stop) at the site of the amber stop signal, respectively (Maruyama et al. 1994, Mikawa et al. 1996).

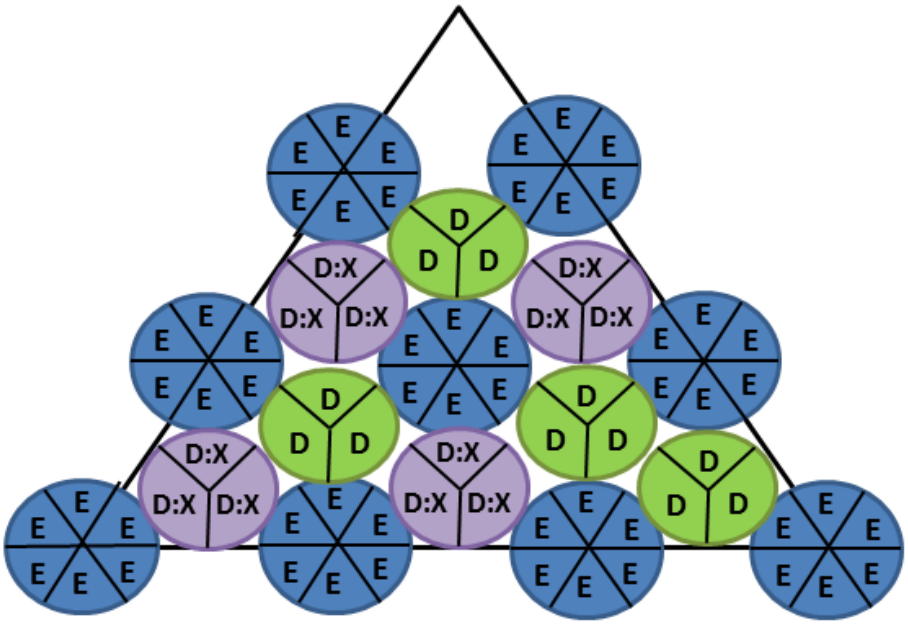

Figure 8: Schematic of controlled phage display on the phage λ capsid. Decoration of the λ capsid under controlled circumstances will result in a display platform, whereby both the fused protein and the wild-type protein are incorporated into the capsid head. The schematic shown here represents a 50% decoration rate. i.e. 50% of the gpD positions are filled with gpD:X fusions labeled "D:X" and 50% are filled with wild-type gpD labeled "D".

1.6 Phage Display Applications

The small-size and the enormous diversity of variants that can be fused to the bacteriophage capsid make phage ideal candidates for numerous applications across many industries. Some primary applications include targeted therapy and detection, and conjugation with macromolecules in medicine, plant science and nanoparticles in materials science (Petty et al. 2007, Willats 2002). Initially, phage display was developed to display random and natural peptide libraries (Dulbecco 1982). Random peptide libraries consist of synthetic random

degenerated oligonucleotide inserts that are used to identify linear antigenic epitopes and offer a universal application base. In contrast, natural peptide libraries that are composed of randomly fragmented DNA from the genomes of selected organisms may be used to identify vaccine components and bacterial adhesins, although most of these clones are nonfunctional (Mullen et al. 2006). Since initial lytic phage display design studies, a great deal of attention has been focused on progressing towards the development of novel therapeutic or industrial applications for the system; recent studies combine the genomic flexibility of phage with phage display to generate genomically modified phage for targeted gene delivery. The list of applications is far too large for a comprehensive review so the following topics have been selected, based on significance and extensiveness in the field.

1.6.1 Phage Vaccines

As vaccine delivery vehicles, bacteriophage vectors offer a strong alternative to the more classical viral and non-viral systems since they possess inherent attributes that permit them to overcome the challenges that generally limit the utility of traditional approaches. The dimensions of phage λ are very similar to many mammalian viruses and may even share some of the same ancestry (Zanghi et al. 2007). They are also endowed with many of the intrinsic mechanisms of mammalian viruses, such as cell entry and endosomal escape, and while perhaps not as efficient as their eukaryotic viral counterparts, these attributes provide an advantage over non-viral vectors (Min et al. 2010). As phage exclusively infect bacteria and are ubiquitous inhabitants of our natural habitat, it is not surprising that they have also been proven to be completely safe in mammalian systems and are free of many of the serious side-effects attributed to mammalian viral vectors (Min et al. 2010, Seow & Wood 2009).

Phage vaccine delivery follows many of the same steps required in the delivery of other non-viral vectors. Research is currently focusing on optimizing the binding and internalization of phage by antigen presenting cells (APCs). However, the mechanism by which phage deliver their DNA cargo to the nucleus once the particle has been internalized is not well understood. It appears that the internalization of targeted phage particles is quite efficient, whereas endosomal escape and nuclear uptake is not (Larocca & Baird 2001). Despite this limitation, phage-based vaccine delivery has been successfully implemented employing two different strategies: i) direct vaccination *via* the manipulation of the phage to display the protective antigen on the surface coat proteins; or ii) using the phage particle as a delivery system for a DNA vaccine expression cassette containing the sequences required for vaccine antigen synthesis packaged into the phage genome (Clark & March 2006, Seow & Wood 2009). (See Figure 9 for a diagram on the examples of phage-based vaccines).

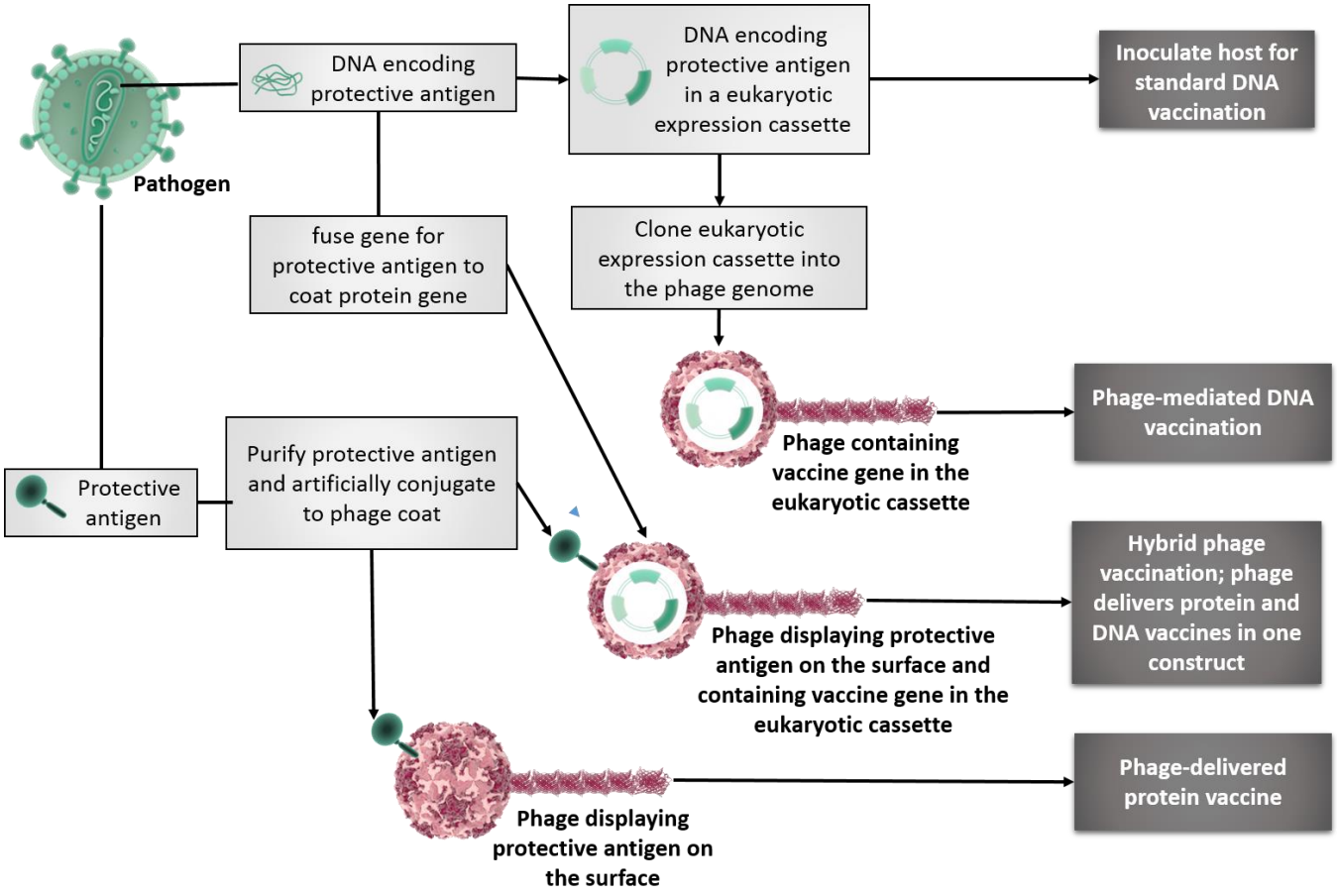

Figure 9: Phage vaccine delivery techniques. There are many ways that phage can be used as vaccine delivery vehicles. It is important to note that the hybrid phage depicted above has been shown to display the protective antigen on the capsid surface; the hybrid phage can display other peptides as well, including targeting peptides designed to increase uptake of the particles. Many phage display techniques can also display multiple peptides on the surface.

The use of phage for targeted DNA delivery offers the inherent advantage of the phage capsid, which can act to protect the DNA within from degradation once it has been injected, thereby acting as a DNA vaccine (Haq et al. 2012). It has also recently been shown that vaccination strategies involving phage carrying DNA are more efficient than naked DNA vaccine strategies (Clark & March 2004, Clark et al. 2011, Haq et al. 2012, March et al. 2004). A potential third strategy combines the above two methods to develop a "hybrid" phage. These phage are specifically engineered to display both the antigen of interest as well as the gene of interest in the genome of the phage for a combined effort. The displayed peptide may also be used as a targeting ligand for the delivery of the phage to specific immune cells and enhance the delivery efficiency (Min et al. 2010; Clark & March 2006; Lankes et al., 2007).

Phage are considered to be natural immunostimulators, where the carrying particle can serve as a natural adjuvant (Clark et al. 2011). This adjuvant effect of phage has been hypothesized to be related to the presence of i) CpG motifs on the foreign phage DNA; and ii) the virus-like repeating structure of the phage coat. It has been demonstrated that the CpG motifs on the phage DNA are likely responsible for the stimulation of the T_h1 immune response in mice when delivered with recombinant Hepatitis B antigen (Malanchère-Brès et al. 2001) and the stimulation of B-cell responses (Clark et al. 2011, Li et al. 2012). Clark *et al*. (2011) demonstrated that phage have an increased antibody response measured after vaccination in comparison to the standard recombinant protein vaccine Engerix for the treatment of Hepatitis B in rabbits. Ling *et al.* (2011) also demonstrated that mice vaccinated with a phage vaccine expressing a DNA expression cassette for the treatment of *Chlamydiphilia abortus*

had higher levels of immune cell and cytokine responses in comparison to those treated with a naked DNA vaccine, although the immune response levels were not as high as those from the attenuated commercial vaccine (Ling et al. 2011). The natural immunostimulatory effect of phage speaks to the potential for phage based vaccines since the phage already possess the natural ability to stimulate an appropriate immune response.

Bastien *et al.* (1997) employed phage fd to display a chimeric protein with a proven protective epitope, G glycoprotein, against human respiratory syncytial virus (RSV), to explore the use of filamentous phage in the development of vaccines. This study showed that mice acquired complete resistance to a viral challenge by the absence of the virus in their lungs and high levels of RSV-specific antibodies. In addition, the level of antibody was only slightly lower than immunized mice with whole RSV virus. This was also the first study that showed recombinant phage can be selected directly from random peptide libraries and then used directly for protection assays (Bastien et al. 1997).

March *et al.* (2004) first employed λ as an encapsulated DNA vaccine where they immunized mice with λ particles encoding either eGFP or hepatitis B surface antigen (HBsAG). The expression system protected the DNA cargo until it was safely within the cell, but these particular constructs did not display the protein on the phage surface (Jepson & March 2004). Both of these modified DNA vaccine constructs were able to elicit an immune response in mice, but results were inconsistent. The group suggested that the display of antigens on the surface of the phage, rather than solely a DNA format, may grant a more specific and effective vaccine approach.

This peptide display approach was realized when Zanghi *et al*. (2005) developed a mosaic expression approach to circumvent the issue of recalcitrance by decorating λ with wild-type and recombinant proteins in tandem. This system utilized two separate plasmid constructs that contained different origins of replication and selectable markers that were co-transformed into a gpD-deficient λ lysogen (Zanghi et al. 2005). When only the recombinant plasmid was expressed, no viable progeny were recovered, indicating that the fusion must either interfere with assembly or prevent formation of stable phage particles. Like wild-type phage, the slight reduction in mosaic phage titers could be attributed to plasmid attributes—mainly copy number and protein expression. With the presence of two plasmids that have theoretically consistent expression and fusion capacities, the level of control is still quite limited.

Thomas *et al.* (2012) recently developed a λ vaccine using a combination of *cis* (*via* recombination) and *trans* (plasmid-mediated) peptide phage display to elucidate how peptide immunization might be superior to genetic immunization. They found that phage-based peptide expression vectors elicited a greater immune response at a physiological pH in higher primates and humans in the absence of an adjuvant than genetic vaccine (Thomas et al. 2012). They also developed a divalent subunit vaccine that was a hybrid of a DNA and a peptide vaccine with two separate fusions to gpD—one with GFP and the other with the TAT protein from HIV-1 that proved to be superior to the peptide vaccine. The TAT protein was specifically chosen for its ability to efficiently deliver to mammalian cells (Eguchi et al. 2001). Both fusions were constructed to the C-terminal of gpD and a short linker was placed between the two protein domains, which were displayed on the phage surface *in tandem*. The

same phage that lacked display for either of these two proteins was used as the DNA vector for comparison. Similar to the system here, the plasmid expressing the fusion was inducible by IPTG and the recombineered genome was passaged through a SupF (Tyrosine) host. In each case, the primary immune response was humoral and λ served as an endogenous adjuvant where the phage that displayed the two peptides outperformed the non-displaying DNA vaccine (Thomas et al. 2012). The preparation process improved as the temperature-inducible promoter used in the system for this research study only required a change in temperature as opposed to chemical inducers.

Hayes *et al.* (2010) developed a λ-based vaccine where the construct had multiple fusions to the C-terminal of gpD—one in which four immunodominant regions of the porcine circovirus capsid were fused, a second with GFP, and the third with a SPA tag protein. Interestingly, the GFP and the circovirus capsid fusions could be expressed constitutively without compromising the viability of the host, while the SPA expression reduced phage viability by more than 50-fold, likely due to recalcitrance. Recalcitrant fusions prevent protein oligomerization and the formation of homotrimers during phage assembly and therefore display fewer D-fusion proteins which compromise phage stability. The circovirus capsid fusions were also able to elicit both cellular and humoral responses in pigs (Gamage et al. 2009, Hayes et al. 2010).

A more recent commercial example of phage display employed λ phage scaffold decorated with HIV-1 envelope protein (Env) via *in vitro* complementation, where the immune response elicited was compared to that of soluble gp140. This strategy was employed because in their native state, envelope spike proteins are sparsely present on the HIV-1 virion

and the ability to increase their density on the phage capsid could in theory generate an improved immune response. Phage were decorated with a mixture (different molar ratios) of gpD:gp140 and wild-type gpD protein. Like Zanghi *et al*. (2005), Hayes *et al.* (2010), and Mattiacio *et al.* (2011) discovered that phage were recalcitrant and unstable when decorated completely with a 20-fold molar excess of fusion protein. They also determined that some fusion proteins could stabilize phage particles even when they only occupy a fraction of the gpD binding sites and that the number of fusions incorporated into the capsid was only 30 copies of Env trimers per particle (Zanghi et al. 2005; Hayes et al. 2010; Mattiacio et al. 2011; Nicastro et al. 2013). As a result, the investigators did not observe an increased immune response to the decorated phage compared to the conventional protein (Mattiacio et al. 2011). Each of these groups also executed codon optimization in developing their constructs, which allowed for more efficient protein expression and less homology of fusions to native λ sequences, thus decreasing the potential for homologous recombination between alleles (Zanghi et al. 2005).

Although phage vectors offer promising advantages, they are not without their limitations. Phage are rapidly removed by the reticuloendothelial system, contain potent antigens (Seow & Wood 2009), and generally offer a lower efficiency of gene delivery relative to their viral counterparts (Larocca & Baird 2001). While these limitations will require further attention, the advantages imparted by phage as single administration gene and vaccine are many and suggest powerful potential for their use in future vaccine development (Seow and Wood 2009).

1.6.2 Phage as Gene Transfer Vehicles

Bacteriophage offer strong potential as gene transfer vehicles, particularly due to the fact that their coat proteins can protect DNA cargo against degradation during delivery (Clark & March 2006, Dunn 1996). Additionally, the tolerance of capsid fusions makes it possible for display phage to target specific cells of choice (Clark & March 2006), a cornerstone of successful gene therapeutic design. Fibroblast growth factors have been used as targeting sequences for the delivery of phage to cells that have the appropriate receptors (Hart et al. 1994, Sperinde et al. 2001). These sequences have been shown to enhance the uptake and endosomal release of phage via proteins such as penton base of adenovirus which mediates entry, attachment and endosomal release (Haq et al. 2012, Piersanti et al. 2004). The transduction domain of HIV (Human Immunodeficiency virus) or the TAT protein, and the Simian Virus 40 (SV40) T-antigen nuclear localization signal have also been exploited to enhance cellular uptake and nuclear localization of lambda phage, respectively (Nakanishi et al. 2003).

The first reported use of filamentous phage for gene transfer and delivery was reported by Hart *et al.* (1994). In this study, phage fd was employed to display a cyclic-binding peptide to the major coat protein pVIII. This N-terminal fusion, occurring at approximately 300 copies/phage particle, was bound to cells and was efficiently internalized. The same peptide sequence was then fused to the major tail protein (gpV) of λ. These modified phage proved to be a more suitable candidate by transfecting mammalian cells at a remarkable frequency in comparison to the controls (Dunn 1996, Hart et al. 1994).

Lankes *et al.* (2007) expanded the application of λ as a gene delivery vector by executing phage-mediated gene transfer *in vivo*. The group constructed recombinant λ particles encoding firefly luciferase (*luc*) in order to visualize gene delivery in real-time via the use of bioluminescence imaging (Lankes et al. 2007). They fused a $\alpha_v\beta_3$ (CD51/CD61) receptor integrin-binding peptide to gpD to increase its uptake by receptor-mediated pinocytosis. This integrin was chosen because it is known to play a role in the binding/internalization in a number of mammalian viruses and it had been used to enhance the targeting of modified viral vectors to dendritic cells. The study showed preferential internalization of fused phage over their non-fused counterparts, where internalization decreased in a dose-dependent fashion.

Vaccaro *et al.* (2006) noted a similar pattern of internalization following the addition of competitor proteins, indicative of a receptor-mediated process. The recombinant phage outperformed the control cells both *in vitro* and *in vivo*. In addition, they noted a 100-fold increase in phage internalization into integrin-positive versus control cells, but only a 3-fold increase in phage-mediated gene expression. This indicated that the level of internalization is not necessarily comparable to the successful delivery of genetic material (Vaccaro et al. 2006). Overall, this study provided a proof-of-concept for the use of recombinant phage to increase the gene transfer *in vivo* and a compelling argument for the use of phage in transgene delivery (Lankes et al. 2007, Vaccaro et al. 2006).

Zanghi *et al.* (2007) explored construct design, where they attempted to improve phage-mediated mammalian gene delivery of a luciferase gene through the simultaneous fusion of proteins to both the head and tail of phage λ. Multiple intracellular barriers such as cell attachment, cytoplasmic entry, endosomal escape, uncoating and nuclear import, must be

overcome for successful gene transfer (Seow & Wood 2009). Multiple peptides could theoretically be displayed *in tandem*, where each peptide could function to circumvent a separate barrier. In addition, the system could potentially target intracellular pathogens to overcome intracellular barriers, where a lower density display would presumably be employed for ligand interaction and receptor-mediated endocytosis, while a higher density display could be used to target a pathogen. The group reported an average number of fusions per phage particle to be ~400 copies/phage particle for gpD and ~100 copies/ phage particle for gpV (Zanghi et al. 2007). The group also supplemented the efficiency of phage-mediated gene transfer in a murine macrophage cell line with the surface display of an ubiquitinylation motif and the system was further improved by the simultaneous tail fusion of a CD40-binding motif (Zanghi et al. 2007).

Sapinoro *et al.* (2008) explored pre-immunization as an approach to increase the uptake of recombinant phage, termed *antibody-dependent enhancement* (ADE). In concept ADE relates to the observation that opsonization, or binding of antibodies to an antigen, permits the more efficient infection of susceptible host cells such as monocytes and macrophage that possess receptors for the antibody isotype. The objective of the group was to develop an *in vitro* model for this phenomenon in mammalian cells by bacteriophage λ vectors and determine their mechanisms. Since it is known that this effect can be mediated through cellular receptors specific for the F_c portion of IgG, the group used a cell line expressing human F_c gamma receptor ($F_c\gamma R$) and found that ADE of phage-mediated gene transfer required the receptor on the surface of target cells (Sapinoro et al. 2008). In addition, prior immunization with wild-type phage resulted in more efficient phage-mediated gene expression in live mice

and this increased transduction was undertaken through a receptor-mediated endocytic mechanism rather than through phagocytosis (Sapinoro et al. 2008). Overall, this research study showed that the system was advantageous toward the development of downstream vaccines and targeted gene therapy approaches.

Although numerous methods have been developed for gene delivery, an efficient platform for protein delivery and more specifically protein delivery *in tandem* with gene delivery does not currently exist. Recently, Tao et al. (2013) developed a T4 DNA packaging machine using T4-based "progene" nanoparticles that were targeted to antigen-presenting cells and were expressed both *in vitro* and *in vivo*. The group fused DNA molecules on the capsid head proteins Soc and Hoc that would later be displayed on the phage heads. Foreign cell penetration peptides (CPPs) and proteins (β-galactosidase, dendritic cell specific receptor 205 monoclonal antibody, and CD40 ligand) were chosen for display onto Hoc. The encapsidated DNA included *GFP* and *luc* (luciferase) genes to enable quantifiable expression within mammalian cells. Overall, the group showed evidence for efficient *in vitro* and *in vivo* progene delivery and expression of self-replicating genes into mammalian cells. Although the results were promising, there is room for further investigation particularly with respect to the *in vivo* studies where, unexpectedly, the strongest luciferase signal came from mice infected with the nanoparticles that did not display a targeting ligand. The authors have attributed this finding to migration of the targeted cells to other parts of the body; an inference that will require further investigation (Tao et al. 2013).

When undertaking a vaccination approach, high-density display may be preferred as functions of the fused protein may not be critical. In contrast, an application such as targeted

gene therapy relies upon ligand interaction and proper folding/function of the fusion to improve cell specificity or enhanced endocytosis. The ability to control the number of fusions provides power and flexibility to cater mosaic phage to different scenarios and needs. Moreover, the ability to control the number of fusions and gpD molecules could reduce the chance of recalcitrance and improve viability. Finally, this system can be expanded to generate multiple fusions and polyvalent therapeutics.

1.6.3 Phage as Bacterial Sensors

There is a strong and growing demand for new technologies that can detect pathogens in food, water, and environmental and patient samples, provided that they can address a real need: i) pathogen detection in food, water or air to identify pathogens or agents of bioterrorism before they can cause harm; ii) diagnose disease early so appropriate therapy can be administered; or iii) identify disease-causing organism(s) to permit preventative measures and detect ongoing outbreaks (Gulig et al. 2008). Classical methods of bacterial detection employed biochemical tests that can be time consuming and require microbes to grow on differential media. More recently, significant efforts have been applied to nucleic acid detection (i.e. real-time PCR) and the use of enzyme-linked immunosorbant assay (ELISA), antibody arrays, fiber optics and surface plasmon resonance to detect pathogens (Gulig et al. 2008). This review will focus on methods that have been developed for bacterial detection using phage reporters; specifically those that utilize phage display technologies.

Bacteriophage-based detection strategies are generally quicker than many antisera/antibody methods, offering results typically in days as compared to months by conventional methods. Phage typing has been most extensively used for the detection of *Mycobacterium*,

Escherichia, Pseudomonas, Salmonella and *Campylobacter* species (Barry et al. 1996). Developing phage reagents is also quite simple, rapid, economical and easy to manipulate genetically. There is a considerable amount of literature from investigations that use phage display methods for the detection of a variety of antigens for a variety of purposes. We will highlight those that contribute a novel aspect to the use of phage display for bacterial detection purposes. The specificity of bacteriophage for bacterial cells enables them to be easily used for the typing of bacterial strains and pathogens. This natural specificity can be improved by phage displaying targeting peptides on the capsid surface. The most commonly used antibody for this is the single chain F variable (scFv) portion that contains the antigen binding regions of the heavy and light chains; an antibody portion can normally be obtained from animals that are immunized with the target antigen/microbe. Phage particles that display the fusion peptide of interest are then selected by a process called "panning", which involves the binding of phage to the antigen, the subsequent washing away of unbound phage, and finally the eluting of bound phage followed by amplification in the appropriate host cell (Smith 1985; Gulig et al. 2008). Unbound scFv is normally unsuccessful for the purposes of bacterial detection.

Sorokulova et al. (2005) developed a random 8-mer landscape phage library expressing fusions to coat protein (pVIII) of fd phage. The phage were panned against *S. typhimurium* whole cells resulting in the isolation of a phage that was highly specific towards *Salmonella* whole cells (Sorokulova et al. 2005). In a follow-up study, Olsen et al. (2006) were able to detect *Salmonella* with this phage at titers as low as 100 cells/mL (Olsen et al. 2006). This technique was also used to pan against *Bacillus anthracis*, an organism of particular

importance in thwarting bioterrorist threats, leading to the identification of multiple phage with the ability to capture anthrax spores with reasonable specificity (Brigati et al. 2004).

Ide et al. (2003) used the New England Biolabs 12-mer library of random peptides in an effort to isolate peptides for the identification of the H7 flagella of *E. coli* O157:H7 (Enterohemorrhagic *E. coli*, or EHEC). This is a pathogenic strain of bacteria that is responsible for the onset of hemorrhagic colitis and hemolytic uremic syndrome (HUS), due to the release of phage-encoded Shiga toxin (H7 antigen) that is shared by most strains and encoded by the resident prophage, 933W. They were able to develop specific clones to H7, one of which could bind to intact *E. coli* cells expressing flagella (Ide et al. 2003). Similarly, Turnbough et al. (2003) developed phage libraries using New England Biolabs 7- and 12-mer libraries to isolate phage clones that could recognize a variety of *Bacillus* spores, including those formed by *B. anthracis* species. They were also able to differentiate between the spore types, an important aspect in the development of anti-spore reagents (Turnbough 2003).

Phage can also be used to deliver reporter genes such as GFP that are expressed upon infection of a bacterium (Loessner et al. 1997; Funatsu et al. 2002). Funatsu et al. (2002) manipulated λ by direct cloning to express a *GFP* reporter gene. The researchers were able to detect an *E. coli* infection four to six hours post-infection, using fluorescent microscopy to detect fluorescing bacteria (Funatsu et al. 2002). In a similar study by Oda et al. (2004), virulent phage PP01 specific to *E. coli* O157:H7 was used. Here, The GFP gene was displayed on the surface of the Soc capsid protein without compromising the phage host range. Visual detection of infected target cells was again accomplished by fluorescent microscopy after an incubation time of only 10 minutes. The test worked on viable cells,

viable but non-culturable, and most notably dead cells, although with a far lower fluorescence level (Oda et al. 2004). The same group constructed a T4-based reporter phage possessing a GFP fusion to the Soc protein of the capsid. This phage mutant was deficient in the ability to produce T4 lysozyme at the end of its replication cycle, thereby trapping the reporter phage within the target cells. Detection and visualization of the targeted cells was relatively efficient as GFP continued to accumulate within (Tanji et al. 2004).

Future applications of phage display to bacterial detection will likely look into the development and utilization of new non-immunoglobulin target-binding tools that can be engineered to increase the randomness of binding. For example: i) affibodies that are small proteins isolated from *Staphylococcus aureus* protein A can be manipulated by randomizing the 13 a.a. binding domain and highly specific affibodies to protphageein targets have already been obtained; and ii) anticalins that are proteins based on lipocalin proteins that transport or store molecules that are soluble and can be manipulated to recognize a variety of targets with high affinity binding (Gulig et al. 2008).

1.6.4 Phage as Bio-control Agents

Expanding on the concept of bacterial detection, phage products can also be manipulated to recognize and clear bacterial infections. Typical phage based bio-control procedures include the use of purified lytic enzymes from phage (Fischetti 2005), while other approaches employ genetically modified phage to not lyse cells, but rather to serve as targeted delivery vehicles for DNA encoding antibacterials, to targeted pathogens (Westwater et al. 2003). Particulate phage are relatively easy and inexpensive to purify, and phage display can also serve as an economical means to purify a particular protein/antibody (Clark & March 2006).

Phage display libraries can easily be screened against a set of target proteins with affinities similar to antibodies, which can then be used as therapeutic agonists or conversely, inhibitors of receptor-ligand interactions (Clark & March 2006). As an added advantage, the generation of phage display antibodies does not require the use of animals when working with existing libraries, eliminating the need to inoculate animals with often toxic substances or highly lethal infectious agents that increase costs and production times (Gulig et al. 2008). Phage display methods can also be performed *in vitro* from randomly generated a.a. sequences or randomly assorted antibody fragments, where the agents can be used directly to determine the detection efficiency (Gulig et al. 2008).

Finally, phage can be used to bind specifically to released components within circulation, including toxins, and bacterial pathogens to prevent them from harming the host (Petrenko & Vodyanoy 2003). An especially novel use of phage display was the nasal administration of phage displaying antibodies against cocaine as a treatment against cocaine addiction (Dickerson et al. (2005). The whole filamentous phage particles were able to effectively cross the blood-brain barrier and penetrate the central nervous system where the specific phage displayed antibodies could bind cocaine molecules, thereby preventing the behavioral effects from the drug (Dickerson et al. 2005).

Phage-based techniques for the control of bacterial pathogens have undergone a great deal of research to date where these methods offer a set of advantages over conventional methods of detection, particularly when considering time and specificity. Furthermore, many of the outlined methods feature high sensitivity and can be offered at relatively low cost. Following administration, phage dissipate rapidly throughout the mammal and reach the organs at

varying rates and to varying degrees (Dabrowska et al. 2005). While this is an advantage for detection and treatment purposes it also means that phage are cleared quickly by the immune system and as strong immunogens, are targets of antibody neutralization and clearance. While phage offer promising alternatives for therapeutic uses, the physicochemical characteristics that make them highly immunogenic, limits their utility as repetitive therapeutics (reviewed in Kaur et al. 2012).

1.7 Summary

With an estimated 10^{31} phage particles worldwide (Gulig et al. 2008), bacteriophage offer a practically unlimited reservoir of exploitable genetic information that can be applied to a plethora of purposes. The applications of phage display are many and the rich and growing research in this area suggests a promising future for their exploitation in medicine, food science, biotechnology and nanotechnology, just to name a few.

2 Rationale, Hypothesis and Objectives

2.1 Rationale

2.1.1 C-terminal eGFP fusions on λ

Bacteriophage λF7 (*λDam15imm21cIts*) was selected as an amber mutant for the gpD gene, whereby the phage develops an immature head lacking gpD that renders it extremely sensitive to EDTA among other irritants and requires external sources of gpD to confer a stable phage capsid head (Sternberg et al. 1979). In this study, C-terminal fusions of gpD were supplied via a 2-dimensional expression system using:

a) The construction of the fusion plasmid pPL451-gpD::eGFP (herein referred to as pD::eGFP). The plasmid was incorporated into high-copy number plasmid vector pPL451 under the control of temperature sensitive repressor, CI857.

b) Amber suppressor strains of *E. coli* which act to read-through the UAG stop codon and insert a particular (and varied depending on the Sup^+ strain) a.a. in its place to allow for the expression full-length wild type alleles of gpD.

2.1.2 Temperature-Inducible control of fusion capsid decoration:

2.1.2.1 First dimension of control - Regulation of *D::eGFP* expression *via* the CI[Ts]857 Repressor:

The fusion protein in plasmid pPL451 is under the control of the temperature-sensitive λ repressor mutant allele, CI857, which acts from λ O_R and O_L operator sites *in vivo* to prevent transcription of prophage genes at low temperatures (<35˚C). Phage λ undergoes induction at higher temperatures where the repressor is inactivated, allowing the development of phage progeny (Figure 10/ Figure 11). In this study, the fusion protein plasmid pPL451 is regulated by a temperature-controlled expression system with CI857 such that:

a) At high temperatures (>35ºC) there is a decrease in CI857 repressor activity permitting the expression of *D::eGFP* fusion from the pPL451 plasmid. This will be seen as both an increase in complementation and an increase in eGFP expression.
b) At low temperatures (<35ºC) the CI857 repressor is active and *D::eGFP* fusion from the pPL451 plasmid is not expressed resulting in decreased gpD::eGFP complementation for the D⁻⁻ mutation, and minimal eGFP λ decoration and activity as compared to higher inducing temperatures.

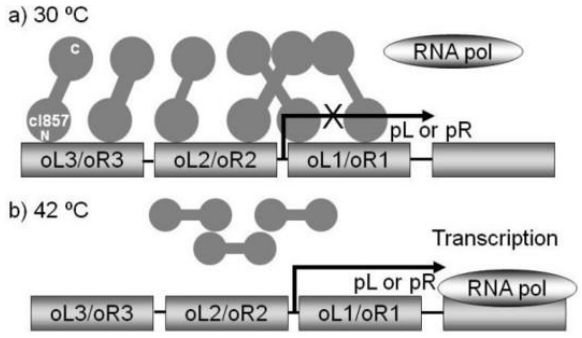

Figure 10: C1857 repressor activity. The λ CI857 repressor maintains the prophage state of the virus at low temperatures by regulating expression via occupation of the λ O_L and O_R operator sites that govern expression of all lytic phage genes (Ptashne 2004).

The λ *cI* gene codes for a repressor that maintains the lysogenic state of the phage. In this study, λ*Dam15imm21cIts* (λF7) was chosen as a λ phage hybrid with the immunity (*imm*) region derived from a closely related, but heteroimmune, lambdoid phage (phage 21) in place of the λ *imm* region, and the remainder of the phage genome derived from λ. Although the λ repressor binds its own operator sites, this hybrid phage possesses the operator sites of phage 21 and is thereby heteroimmune and not regulated by λ CI.

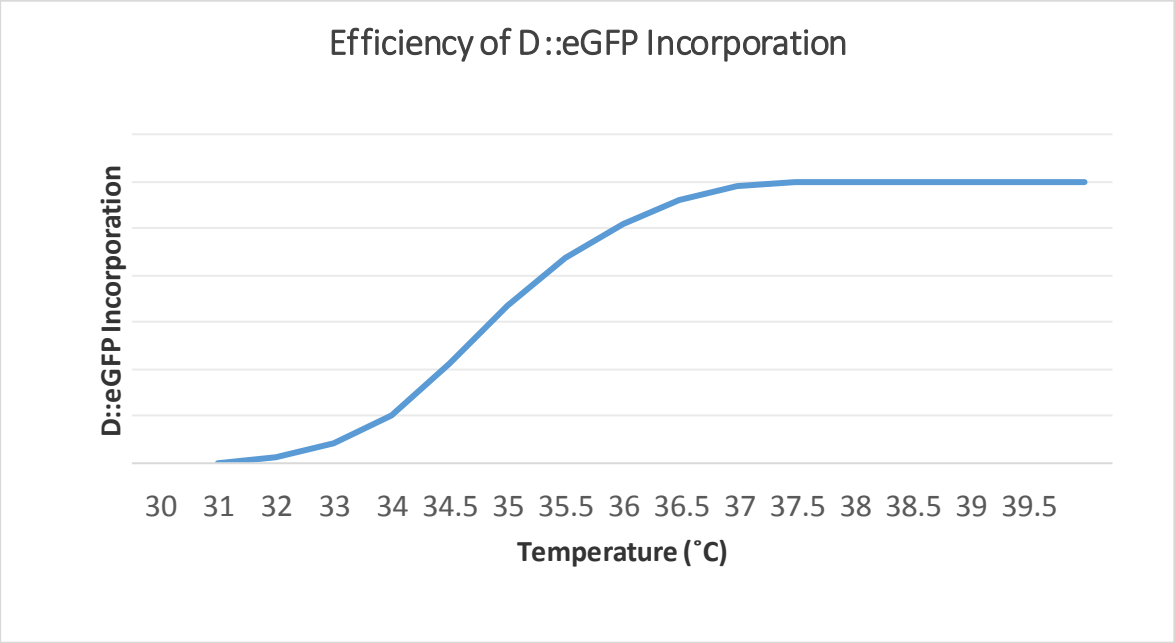

Figure 11: Hypothetical efficiency of gpD::eGFP incorporation with pPL451 gpD::eGFP. The fusion protein is under temperature control where at 35˚C, we will begin to see the derepression of the pPL451 plasmid and with that increasing incorporation of gpD::X fusions per λ phage capsid, maximized at 405 to 420 possible incorporations per capsid.

2.1.2.2 Second-Level of Control—Amber suppression and the generation of different alleles of gpD:

The phage employed in this work is the λ amber mutant, λ*Dam15imm21cIts*, or λF7. This phage encodes an amber (UAG) mutation at the 68th a.a. position of *D* that imparts the early termination of the translation of the *D* transcript. In wild-type (suppressor-negative, or Sup$^-$) *E. coli* hosts, the *Dam15* yields terminated translation and the generation of a 67 a.a. truncated gpD product, precluding the ability of λF7 phage to form stable capsids necessary to produce viable progeny. The fusion plasmid (pPL451 gpD::eGFP) encodes the *D::eGFP* fusion, thereby providing the only source of functional gpD in Sup$^-$ cells to be incorporated into the phage capsid.

E. coli amber suppressor (Sup$^+$) strains permit the full translation of *Dam15* transcripts and allow for the formation of various full length gpD capsid protein as each amber suppressor encodes a different mutated tRNA gene that reads the UAG stop codon and inserts a residue in its stead (Figure 12). The double amber suppressor, BB4 (*supE, supF*), can yield functional λF7 phage particles in the absence of the fusion plasmid and thus can serve as a positive control for phage efficiency of plating, as well as a negative control for eGFP decoration. Amber suppressor strains W3101 SupD (*serU132)*, W3101 SupE (*glnV44)* and W3101 SupF *(tyrT5888)* insert amino acids serine, glutamine and tyrosine in place of the amber stop codon and conferring alleles gpDQ68S, gpD$_{wt}$ and gpDQ68Y, respectively. We hypothesized that suppressor SupE, yielding gpD$_{wt}$ would confer the strongest suppression as it restores the pristine gpD sequence. SupD and SupF were hypothesized to develop alleles of gpD that would be less stable, and therefore less favourable for capsid head development.

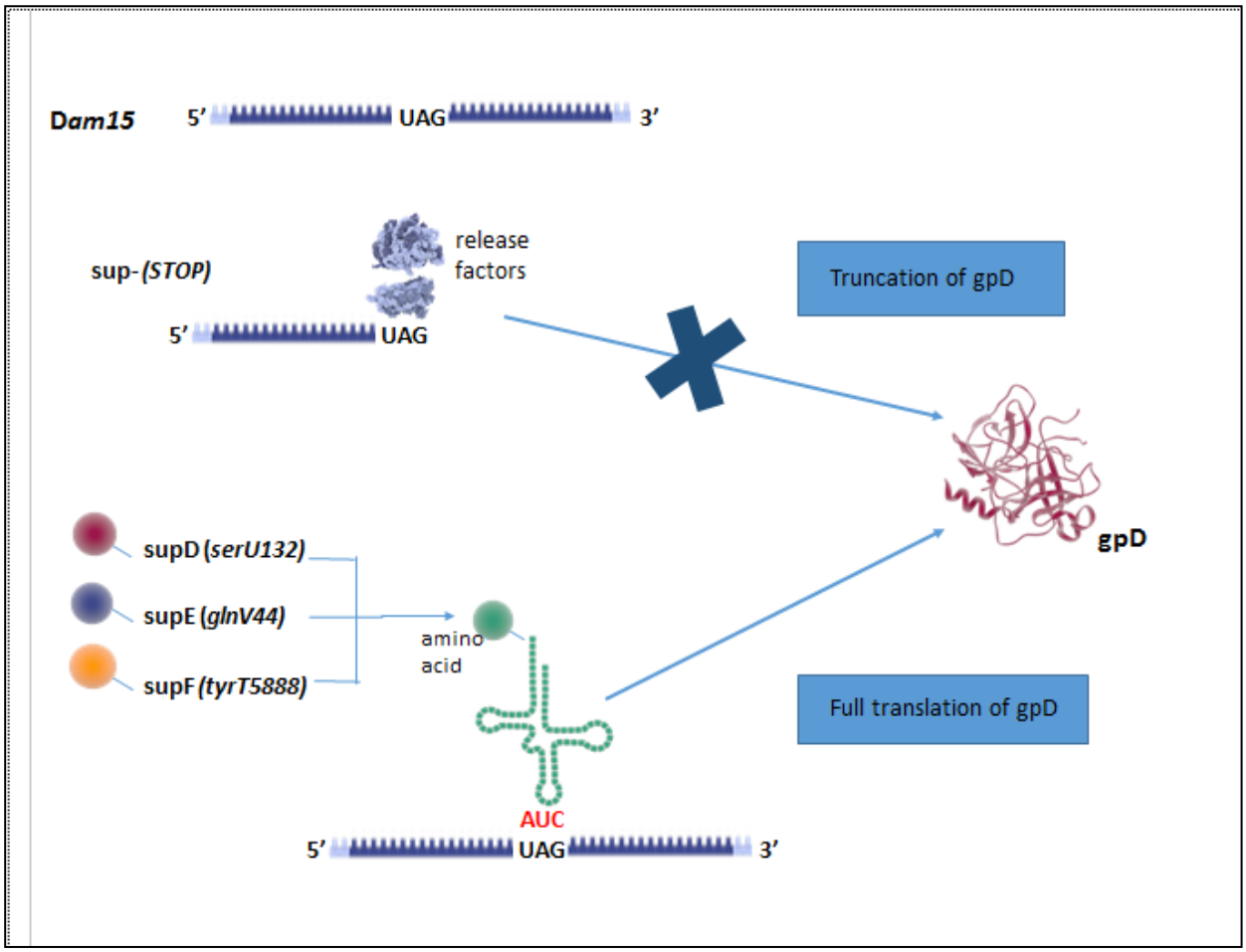

Figure 12: Amber suppressor strains. The amber suppressors act on the stop codon (UAG) in the sequence of the phage gene for gpD and use a tRNA which substitutes an a.a. for the stop codon resulting in the full translation of wild-type alleles of gpD. Strains that do not contain an amber suppressor mutation will end up with a 67 a.a. truncated gpD protein due to translational stop at the 68th position translational stop encoded by the amber mutation.

2.2 Hypothesis

By varying the temperature and the level of suppression of λF7 (*λDam15imm21cIts*) phage grown in an *E. coli* host species, the number of gpD::X fusions decorating phage λ can be varied in a predictable and consistent manner, whereby the degree of decoration will depend on the size of the intracellular fusion protein pool available, and the functionality of the various full length alleles of gpD present. This will be seen across two levels of control, where:

a) Raising the temperature will result in an increasing incorporation of gpD::X fusions per λ phage capsid
b) There will be a functional variance amongst the full length gpD alleles where the structural functionality of alleles will be inversely proportional to the number of fusion decorations on the phage capsid.
c) The combination of the genetic control mechanisms will permit a robust spectrum of gpD::X decorative permutations on average per λ phage capsid.

2.3 Objectives

The objectives of this research address the bacterial and bacteriophage preparations as characterization of the preparation permutations:

1. To prepare phage samples under various temperature and isogenic suppressor conditions, generating a robust sample set to assess regulate adjustability of fusion decoration.

2. To determine the ability of various gpD alleles and fusions to complement for the *Dam15* mutation, as a measurement of phage viability.

3. To determine the average number of gpD::eGFP peptides/phage capsid under each set of these conditions. To determine the relative size and the surface complexity of the phage preparations under each condition.

4. To assess phage stability of the phage fusion preparations, under each set of conditions.

A diagram of the combination of the levels of control can be found in Figure 13 (below).

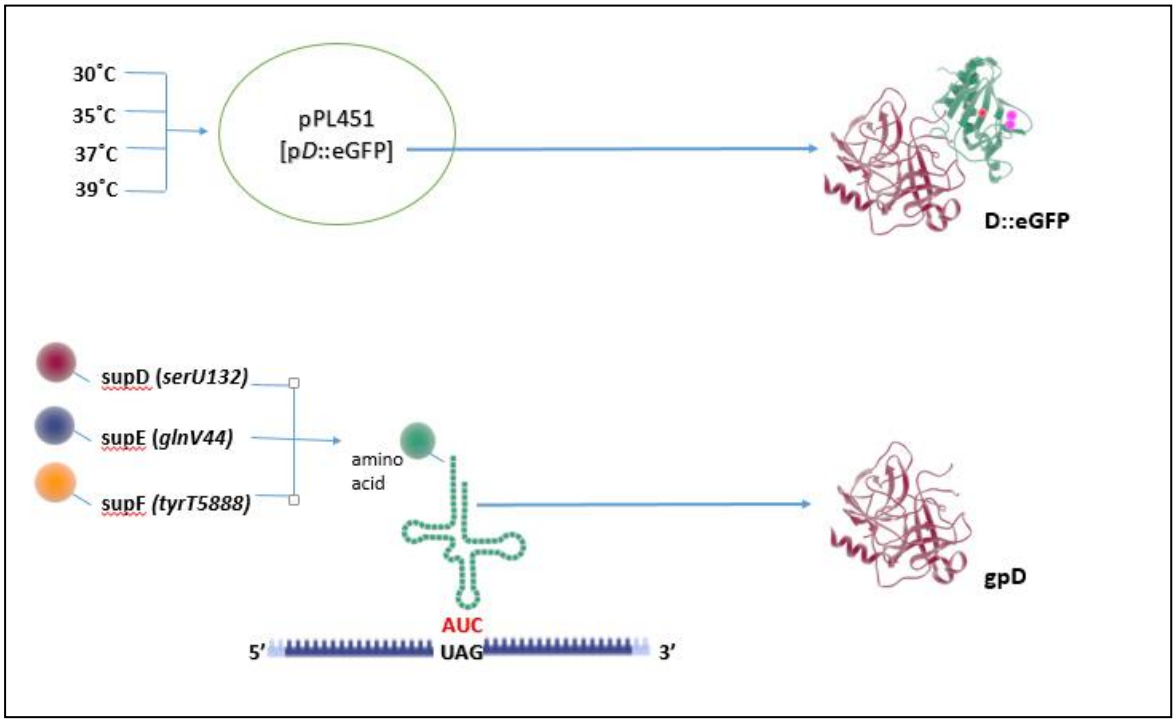

Figure 13: The dual expression system. The combination of the genetic control mechanisms will permit the availability of both gpD and fusion protein D::eGFP within the cell to decorate the phage capsid head. The fusion protein is under temperature control, such that an increase in temperature will result in an increasing incorporation of gpD::X fusions per λ phage capsid. Each full length gpD allele, different for each suppressor strain, will vary in its functionality and this functionality will be inversely proportional to the number of gpD::eGFP fusions averaged per phage capsid.

3 Materials and Methods

3.1 Buffers and solutions

Ampicillin Stock (Sigma Aldrich, Oakville, Canada)

Purpose: A selective marker necessary for plasmid amplification and maintenance of pPL451 and derivative plasmids in *E. coli* hosts. .

Prepared at a concentration of 50mg/mL by dissolving ampicillin stock powder into sterile water and filter sterilized.

Stored at -20º C; thawed solution was added to media as necessary to final concentration of 100 μg/ml.

Luria Bertani (LB; BD Difco, Mississauga, Canada) Broth

Purpose: a nutrient-rich broth used for the rapid growth of bacteria cultures in culture.

1L ddH_2O added to: 10g Tryptone, 5g Yeast abstract, 5g NaCl.

Antibiotic was added as needed to agar after autoclaving.

Stored at room temperature (4˚C if antibiotic added)

LB Agar (BD Difco, Mississauga, Canada)

Purpose: Used for the growth of bacterial cultures on semi-solid media (plating)

1L ddH_2O added to: 10g Tryptone, 5g Yeast abstract, 5g NaCl, 13g bacto agar

Antibiotic was added as needed to agar after autoclaving. Autoclaved media was poured to sterile monoplates and stored at 4˚ C.

LB Top Agar (BD Difco, Mississauga, Canada)

Purpose: Used for the even dispersion of bacterial growth cultures as a plate overlay.

1L ddH_2O added to: 10g Tryptone, 5g Yeast abstract, 5g NaCl, 7g bacto agar

Aliquots were dispersed into bottles then autoclaved as necessary and stored in 52˚ C water bath.

PEG (Polyethylene Glycol) (Sigma Aldrich, Oakville, Canada)

Purpose: used for phage concentration and purification.

1L ddH_2O added to: 0.2 M PEG 8000, 0.15 M NaCl and filter sterilized.

TN Buffer (Fisher Scientific, Ottawa, Canada)

Purpose: used for phage dilutions and storage.

1L ddH_2O added to: 0.1 M NaCl, 0.01 M Tris-HCl, pH adjusted to 7.8 and stored at room temperature after autoclaving.

TN/EDTA Buffer (Fisher Scientific, Ottawa, Canada)

Purpose: used for phage EDTA sensitivity testing.

1L ddH_2O added to: 0.1 M NaCl, 0.01 M Tris-HCl, pH adjusted to 7.8 + 0.1 M EDTA and stored at room temperature after autoclaving.

3.2 Strains and plasmids

Strains of bacteria, phage and plasmids used in this work are shown in Table 1.

Table 1: Summary of Bacteria, phage and plasmids in this study

Cell/Phage/Plasmid Designation	Genotype	Source/Reference
Bacterial Strains		
BB4	*supF58 supE44 hsdR514 galK2 galT22 trpR55 metB1 tonA* DE(*lac*) U169	Agilent Technologies, Inc.
W3101	F-, *galT22, λ-, IN(rrnD-rrnE)1, rph-1*	CGSC #4467 Bachmann (1972)
W3101 SupD	F-, *galT22, λ-, IN(rrnD-rrnE)1, rph-1, uvrC279::Tn10, serU132*(AS),	Nicastro et al. (2013)
W3101 SupE	F-, *galT22, λ-, IN(rrnD-rrnE)1, rph-1, crcA280::Tn10, glnV44*(AS),	Nicastro et al. (2013)
W3101 SupF	F-, *galT22, λ-, IN(rrnD-rrnE)1, rph-1, oppC506::Tn10, tyrT5888*(AS)	Nicastro et al. (2013)
Phage Strains		
λ*imm*21	λ*imm21cIts*	Windass & Brammar (1979)
λF7	λ*Dam15imm21cIt*s	Mikawa et al. (1996) Maruyama et al. (1994)
Plasmids		
pPL451	*pM-cI857-pL-cI857-pL-MCS-tL*	National BioResource Project (NBRP);
pPL451 gpD	*pM-cI857-pL-cI857-pL- D-tL*	Sokolenko et al. (2012)
pPL451 gpD::eGFP	*pM-cI857-pL-cI857-pL- D::gfp-tL*	Sokolenko et al. (2012)

3.2.1 Bacterial Strains

BB4 (*supF58 supE44 hsdR514 galK2 galT22 trpR55 metB1 tonA* DE(*lac) U169)* was utilized as a positive control as the baseline for the determination of the efficiency of plating (EOP) of each of the amber mutant phage (λF7) samples. BB4 served as the 100% plating efficiency standard from the action of dual amber suppression (*supE and supF*) encoded by this strain. Plating efficiency of the λ*Dam15* mutant on this strain is comparable to that of the wt λimm21 phage.

W3101 served as the negative control for λ*Dam15* plating efficiency (EOP) as well as the host strain of the negative control phage (λF7) sample. This strain is free of an amber suppressor (Sup^{-}) λ*Dam15* is phenotypically D^{-} on this host and inviable.

Isogenic suppressor (Sup^{+}) strains of W3101 (F-, *galT22, λ-, IN(rrnD-rrnE)1, rph-1*) were previously constructed in our lab in two steps (Sheldon 2013). First, P1 *rev6*-mediated transduction of a tetracycline resistance (Tc^{R}) marker from CAG12077 to recipient amber suppressor (AS) strains DS-3 (F-, *phoA4(Am), serU132(AS), his-45, rpsL114(strR), valR116),* and W3899 (F-, *glnV44(AS), nadB7*) was performed to link the AS marker to the Tc^{R} marker. K1227 (SupF) already possessed a linked Tc^{R} marker (see Table 1). P1 *rev6* was used to co-transduce the AS and Tc^{R} marker (<2 min distance) into recipient W3101 cells, which were screened with λ*Dam15imm21cIts* (λF7) and λ*Sam7* phage to ensure transfer of the AS alleles, respectively linked to the Tc^{R} marker, derived from donor strains, to the W3101 non-suppressor (Sup^{-}) recipient strain. The amber suppressor mutants used in this study were: W3101 SupD (*serU132),* W3101 SupE (*glnV44)* and W3101 SupF *(tyrT5888).*

3.2.2 Phage Strains

λF7 (λ*Dam15imm21cIts*) was used as the lambda *D* amber mutant phage which is unable to form viable phage particles in the absence of amber (UAG) stop codon suppression at position 68 of the 110 a.a. protein. The viability, stability and analysis of capsid fusions were all studies on this phage under a variety of conditions.

λimm21 (λ*imm21cIts*) was used as a control for sizing experiments with dynamic light scattering. This phage is structurally and genetically identical to wild-type phage λ except for the immunity which has been recombined with the immunity region of phage 21.

3.2.3 Plasmids Used

pPL451-gpD::eGFP (pD::eGFP) involved the *gpD::eGFP* expression from this multicopy plasmid (pPL451; Figure 14) governed by a temperature-sensitive allele of the λ CI857 repressor. The *D::eGFP* sequence designed creates a C-terminal eGFP translational fusion with λ *D* capsid gene, separated by an in-frame short linker a.a. p(TSGSGSGSGSGT) followed by a *Kpn*I cut site to allow for removal and exchange of *eGFP*.

Plasmid pPL451-gpD (pD) was constructed by digesting pPL451-gpD::eGFP by *Kpn*I removing all but the last 30 C-terminal bp of *eGFP*. Plasmid pPL451 was digested with *Hpa*I and pPL451 *gpD::eGFP* and pPL451 *gpD* were double digested with *Hpa*I and *Nco*I and the digestion pattern was analyzed to ensure cloning accuracy.

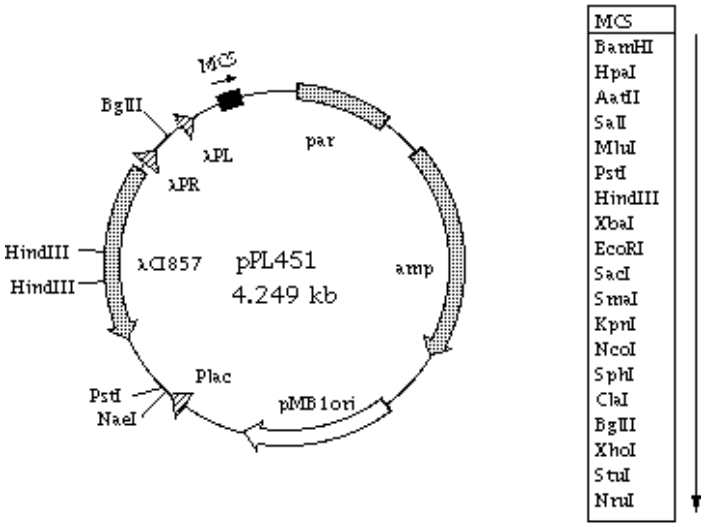

Figure 14: Plasmid pPL451. This 4.249 kb temperature regulated expression vector is driven by λ P_L promoter under the control of the temperature-sensitive CI857 repressor encoded by the cI857 gene that stimulates its own expression.

3.3 Lysate Preparation and Amplification

Cultures of transformed W3101 Sup^+/Sup^- [pPL451-gpD::eGFP] (pD::eGFP) *E. coli* cells were grown on plates at 30, 35, 37 or 39°C overnight, while cultures of W3101 [pPL451-gpD] (pD) were grown up at 37°C only, prior to the addition of primary lysate dilutions. 1:10 dilutions of primary lysates were prepared in 1 mL of TN buffer (0.01 M Tris-HCl and 0.1 M NaCl, pH 7.8, (Fisher Scientific, USA). Lysate dilutions were added to 0.3 ml of cells, incubated for 2 h at experimental temperature prior to adding 3 ml of top agar (Bacto Tryptone and Bacto Agar from Difco Laboratories, Sparks, MD) and plates were incubated overnight at the experimental temperature. Plate lysates were then prepared by adding 10 mL of TN buffer to the surface of the plate, incubating for 8 h at 4°C, then transferring solution and top agar to a conical tube, mixing and centrifuging at 12 K RPM (Avanti J-E Centrifuge, Beckman Coulter, Mississauga Canada) at 4°C for 20 min.

3.4 Phage Purification

To remove cellular debris, lysates were then filtered through a sterile 0.45 μm syringe filter (BD Discardit, India). To purify lysates from unincorporated fusion and other cellular proteins, particularly unincorporated gpD::eGFP, lysates were purified as previously described by PEG precipitation and gel chromatography offering lysate purity comparable to that of CsCl centrifugation and amenable to lysate smaller volumes (Zakharova et al. 2005). Lysates were concentrated through PEG precipitation, as previously described (Baker Laboratory 1999), then disseminated through a 50-150 μL agarose size exclusion column (4% beads, ABT, Spain) in buffer containing 10 mM Tris-HCl (pH 7.5) and 1 mM $MgCl_2$. Samples were stored at 4ºC.

3.5 Phage Titration and Efficiency of Plating Assays

Phage were titered at each step of purification by standard viability assays by standard plaque forming unit assay using fresh BB4 *E. coli* cells as the 100% control, as this strain repeatedly generates highest titers of λF7 ranging from 10^{10} to 10^{12} phage/ml. Plates were incubated overnight at experimental temperature when necessary, otherwise, at 37ºC. Relative EOPs at all test temperatures were determined as phage plating efficiency on the experimental strain divided by that scored on the BB4 100% control.

3.6 Dynamic Light Scattering of Phage

Phage particle size was measured at 25ºC using a Malvern Zetasizer Nano ZS instrument (Malvern instruments, UK). Samples were prepared in Milli-Q water and filtered using a 100 nm filter prior to measurement. The measured sizes are reported using a percent intensity

distribution. Each data point was automatically repeated in triplicate, and the average was reported. Sizing results are expressed based on "X" increase compared to wild type, which is λ*Dam15imm21cIts* (λF7) grown on the BB4 providing suppressed dual gpD_{wt} and gpDQ68Yincorporation into the resultant phage capsid.

3.7 Whole Phage Fluorimetric Analysis

Phage samples were prepared in TN buffer by diluting each sample to a uniform concentration of 2.0 x 10^9 PFU/mL. 150 µL of each prepared sample was then added to a sterile 96 well plate (Starstedt) and were analyzed using a SpectraMax M5 spectrophotometer at an excitation of 485 nm and an emission of 555 nm. The data was analyzed using the SoftMaxPro V5 software where each well was set to be automatically read 6X and the samples were run in duplicate with the average being reported. Phage samples were run alongside an eGFP purified protein standard (Cell Biolabs Inc. #212103) to determine the protein concentrations of each sample. Phage fluorescence for each preparation derivative was interpolated from the trend-line for known eGFP concentrations and the standard error was determined by finding the error associated with this interpolation. The standard error of each of the sample fluorescence values was determined in a weighted analysis against the determination of the sum of the squares of the fluorescence based deviations from the trend-line curve of the fluorescent standard. The standard deviation of each sample was not taken into consideration in the calculations as these deviations were determined to be statistically less significant than the determination from the interpolation itself.

3.8 Flow cytometry analysis

Fluorescence and side scatter measurements of phage samples were determined on a FACSCalibur flow cytometer (BD Biosciences, San Jose, CA) as described by Sokolenko et al. (2012). Briefly, the flow cytometer was equipped with a 15 mW air-cooled argon-ion laser, with an excitation frequency of 488 nm. Side scatter (SSC) and Fluorescence (FL) photomultiplier tube (PMT) voltages were set to 500 V and 525 V, respectively, with logarithmic amplification. A 530/30 nm bandpass filter was used for the observation of *D::eGFP* fluorescence. All samples were serially diluted 1X, 10X, and 100X using phosphate buffer saline (PBS) and run for 30 s at the low flow setting (20 μL/min). The dilutions were used to assess instances of "coincidence", where a high sample concentration results in multiple particles being observed as a single event. Data analysis was conducted by Stanislav Sokolenko (UW, Chemical Engineering) as described in Sokolenko et al. (2012).

3.9 EDTA sensitivity

Phage were diluted in TN buffer (0.01 M Tris-HCl and 0.1 M NaCl, pH 7.8) (Fisher Scientific, USA) to a universal concentration of 4.0 x 10^8 PFU/mL, then were diluted 100-fold into TN/EDTA buffer (0.01 M Tris-HCl (pH7.8), 0.1 M NaCl, and 0.01M EDTA) and incubated for 25 min at 23^{o}C. EDTA inactivation was stopped by diluting the samples 100-fold into TN buffer and immediately plating the mixture on BB4 cells (*SupE, SupF).* Plates were incubated overnight at 37^{o}C. Relative plating efficiency of each sample was determined by measuring phage relative plating efficiency divided by the original phage titer as the 100% positive plating control.

Chapter 4 : Results

4 Results

4.1 Suppressor conferred alleles

To identify the ability of different amber suppressors to reverse the λF7 (λ*Dam15imm21cIts*) lethal *Dam15* mutation, an isogenic set of amber suppressor derivatives of W3101 (Sup$^-$) was generated and the plating efficiency of λF7 was assayed on each suppressor host strain (Table 2). Of the three different gpD alleles generated *via* suppression, gpDQ68S, generated by the SupD host, was least effective in complementing the *Dam15* mutation and improved viability by only 10-fold compared to that of the Sup$^-$ control at 37^{o}C. In addition this allele imparted pinpoint plaques on the SupD strain, indicative of a very low burst size of viable progeny. In contrast, the gpD_{wt} allele, conferred by the SupE strain, restored viability to about 10% that of the double suppressor (SupE, SupF) positive (designated 100% plating) control. The gpDQ68Y allele, imparted by the SupF strain, also surprisingly performed as well, if not marginally better than SupE in an otherwise isogenic host background. The gpDQ68Y allele restored viability to about 20% that of the positive control, despite the size and polarity difference between glutamine (SupE) and tyrosine (SupF). These results were corroborated by the efficiency of plating (EOP) on hosts carrying the parent (backbone) plasmid, pPL451, indicating that suppressor capability was not dramatically impacted by differences in temperature, nor by the presence of the CI857 repressor (Table 2).

Next, we sought to determine the ability of the pD and pD::eGFP plasmids to complement for the *Dam15* mutation of λF7. The expression of the *D* allele or *D::eGFP* fusion in these plasmids, respectively, is governed by the temperature sensitive λ CI857 repressor. First, the non-suppressor strain W3101 was transformed by pD and pD::eGFP, assuming that the ability to properly package and produce viable λ*Dam15* particles would rely solely upon *in trans* complementation for the *Dam15* mutation from the plasmid. As expected, at increasing temperatures, complementation for *Dam15* by plasmid-borne *D* (pD) increased as repressor activity decreased, with optimal results seen at 39°C, where near full viability of λ*Dam15* was restored (Table 2). The lack of complementation by pD at 30°C resembled that of pPL451 (D^{-}), indicating strong repression and insignificant promoter leakiness. The experimental plasmid expressing *D::eGFP* also showed a temperature-governed complementation profile that paralleled that of the pD plasmid, despite that viability was about 10-fold lower at all assayed temperatures, where optimal complementation was achieved again at 39-40°C. In contrast, as expected, the D^{-} parent plasmid (pPL451) was unable to complement for the mutation at any tested temperature.

Complementation for the *Dam15* mutation by the gpD and gpD::eGFP plasmids could not be differentiated from suppression of the mutation on SupE (gpD_{wt}) and SupF (gpDQD68Y) hosts carrying the plasmid due to strong suppressor activity by these strains at all temperatures. However, due to the low viability of λ*Dam15* on the SupD derivative, complementation by gpD::eGFP was observable as expression of the fusion increased with rising temperature and like the Sup^{-}[pD::eGFP] strain, SupD[pD::eGFP] provided the

greatest and a similar level of complementation for the *Dam15* mutation at 39-40ºC. Plaques also were observed to increase from pinpoint to wild type λ plaques on this host.

Table 2: Variable amber suppression and complementation of the Dam15 mutation

Strain [1] / Plasmid [2]	**Relative efficiency of plating (EOP) [3]**				
	30º C	**32-33 º C**	**35 º C**	**37 º C**	**39-40 º C**
Sup-	---	---	---	1.92×10^{-6}	---
pD⁻	4.06×10^{-6}	5.0×10^{-6}	$3.1x\ 10^{-6}$	1.7×10^{-6}	2.0×10^{-6}
pD⁺	7.5×10^{-6}	3.2×10^{-5}	2.1×10^{-4}	0.15	0.93
pD::eGFP	7.5×10^{-6}	2.0×10^{-5}	2.0×10^{-5}	0.02	0.01
SupD	---	---	---	1.13×10^{-5}	---
pD⁻	8.8×10^{-5}	6.5×10^{-5}	1.5×10^{-5}	9.5×10^{-6}	2.3×10^{-5}
pD::eGFP	4.9×10^{-5}	1.8×10^{-5}	8.0×10^{-5}	0.09	0.05
SupE	---	---	---	0.09	---
pD⁻	0.04	0.11	0.07	0.03	0.08
pD::eGFP	0.1	0.04	0.02	0.07	0.03
SupF	---	---	---	0.19	---
pD⁻	0.01	0.01	0.04	0.04	0.03
pD::eGFP	0.1	0.13	0.06	0.07	0.05

[1] Derivatives are W3101 background.

[2] Derivatives of CI857 temperature-regulated expression plasmid, pPL451.

[3] All EOP determinations are averaged from a minimum of three assay and determined using BB4 (SupE, SupF) as the designated full (100%) plating control.

4.2 Fluorimetric Analysis of gpD::eGFP decorated phage

λ*Dam15* phage were variably decorated with gpD::eGFP by passaging through the Sup$^-$ and Sup$^+$ strains carrying the pD::eGFP plasmid at various temperatures. All lysates were standardized for titer before being assayed for functional fluorescence by fluorimetry. Emitted fluorescence from 10^8 phage from each lysate was interpolated against an eGFP standard of known concentration, and the average number of eGFP fusions per phage was then determined (Table 3/ Figure 15). Due to the expected lack of production of a functional gpD allele from either the phage or the plasmid at 30^{o}C in Sup$^-$ [pD::eGFP], no progeny can be formed and as such lysates could not be generated under this condition. Upon raising the temperature to >35^{o}C, the *D::eGFP* fusion was expressed to yield some viable phage and to produce a lysate. Decoration of phage by eGFP was increasingly evident with rising temperature (derepressing expression of *pD::eGFP*) above 35^{o}C, with greatest fluorescence observed at 37^{o}C. All lysate preparations similarly showed increases in fluorescence up to 37^{o}C, albeit considerably lower for phage prepared on the strong suppressor strains, SupE and SupF. This finding is attributable to the preferential packaging of gpD$_{wt}$ or gpDQ68Y alleles compared to gpD::eGFP fusion proteins during phage capsid assembly. In contrast, lysates prepared on SupD, offering the weakest gpDQ68S suppressor, imparted the strongest fluorescence signal from all preparations, with minor but notable fluorescence even at 30^{o}C. The signal observed at this temperature suggests that some leaky expression of *pD::eGFP* from the plasmid must occur under repressing conditions (30^o), but more importantly demonstrates the strong ability of gpD::eGFP to complement *Dam15* in the presence of the

poorly functional gpDQ68Y protein. We noted quite high variability between readings for SupD prepared lysates at most temperatures, suggesting that despite generating the highest possible incorporation of gpD::eGFP into the phage, decoration between phage prepared on this strain are inconsistent, or may result in multiple preferred decorative species. We discuss and offer an explanation for this finding below.

Interestingly, lysates prepared at 39-40^{o}C on all strains offered decreased fluorescence compared to those prepared at 37^{o}C on all Sup^{+} and Sup^{-} strains, despite that derepression of *pD::eGFP* at this temperature is complete and offered highest complementation efficiency for the *Dam15* mutation. To further investigate this finding and determine whether this is due to diminished activity of eGFP at 40^{o}C, or rather decreased integration of gpD::eGFP into the phage capsid, we next sought to examine the size of resultant decorated phage.

Table 3: Estimated average eGFP molecules per phage

Strain (+/- Plasmid) [1]	**Estimated eGFP/phage [2]**			
	30°C	**35°C**	**37°C**	**39°C**
Sup⁻ [pD::eGFP]	n/a	44 ± 4	115 ± 4	61 ± 4
SupD [pD::eGFP]	86 ± 4	127 ± 4	147 ± 4	142 ± 4
SupE [pD::eGFP]	46 ± 4	53 ± 4	77 ± 4	69 ± 4
SupF [pD::eGFP]	65 ± 4	69 ± 4	89 ± 4	69 ± 4

[1] all strains are derivatives of W3101.

[2] fluorescence measurements were divided by those derived from λF7 grown on that strain. Values in parentheses denote calculated number of functional eGFP fusions per phage interpolated from eGFP purified protein fluorescence calibration curve.

[3] Phage preparation on W3101 [pD] at 37°C expressing gpD_{wt} *in trans*

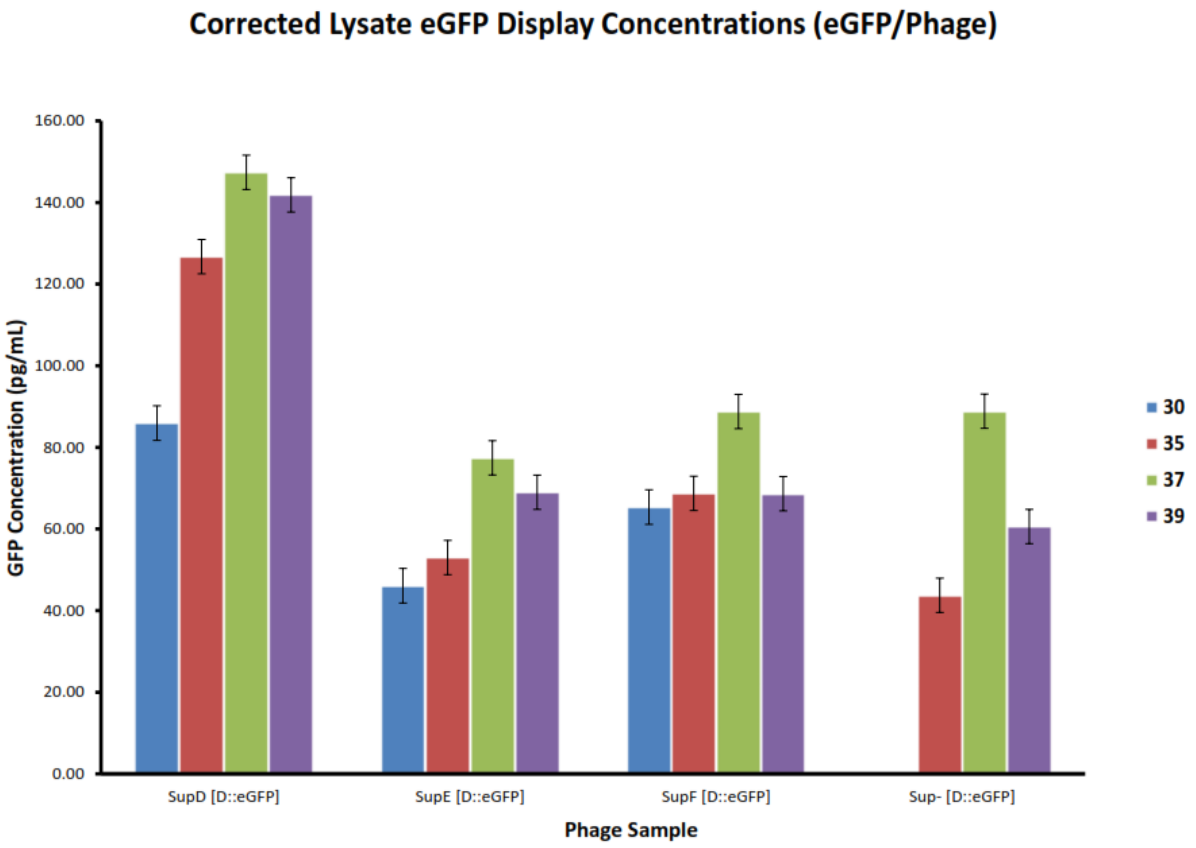

Figure 15: Separation of decorated lysate preparations based on fluorescence emitted. Fluorescence ratios based on comparison to λF7 (λ*Dam15*) grown on W3101 SupE [pD::eGFP]. Measured fluorescence data was analyzed using the SoftMaxPro V5 software based on 6 readings and the samples were run in duplicate with the average being reported. Phage samples were run alongside an eGFP standard to determine the protein concentrations of each sample. Phage fluorescence for each preparation derivative was interpolated from the trend line for known eGFP concentrations. The data was corrected against the W3101 Sup⁻ [pD] negative control where the difference of this fluorescent data point was subtracted from each sample. The data was corrected against the W3101 sup- [pD] negative control where the difference of this fluorescent data point was subtracted from each sample.

4.3 Size comparisons of gpD::eGFP decorated phage

Lysates prepared on the Sup series at experimental temperatures were standardized for titer and then sized by dynamic light scattering (DLS) to approximate relative size differences between undecorated and decorated fusion (gpD::eGFP) displaying phage (Figure 16). The size determinations for λ*Dam15imm21cIts* (λF7) phage grown on SupE, (gpD_{wt}), compared well to that of λimm21 (D^+ parent of λF7) and was used as the wild type phage size control, generating phage with an average diameter of 62 nm. Relative size differences between λ*Dam15* phage grown on the suppressor host series at 37ºC in the absence of gpD::eGFP, was first determined. As expected, phage grown on Sup⁻ [pD] cells at this inducing temperature were similar in size to the control due to efficient complementation, while SupD (gpDQ68S) preparations in the absence of pD were surprisingly only about a third the size. This finding may suggest that the gpDQ68S allele incorporates very poorly into the capsid, resulting in the smaller capsid size. Next, λ*Dam15* phage preparations passaged through the suppressors carrying the gpD::eGFP plasmid at various temperatures, were sized by DLS in triplicate and compared to the size of the undecorated control phage grown on SupE in the absence of pD::eGFP (Table 4/ Figure 16). In all cases, phage size grew as temperature incrementally increased up to 37ºC, where expression of *pD::eGFP* was increasingly derepressed. Interestingly, phage samples prepared at 39º–40ºC, where *pD:eGFP* expression should be maximal, indicated a 30 to 40% decrease in phage diameter compared to that at 37ºC, suggesting that either fewer gpD::eGFP were incorporating into the capsid, despite complete derepression of *pD::eGFP,* or that eGFP were being shed from the decorated phage. Phage prepared on SupD [pD::eGFP] at 37º and 39ºC were particularly interesting

however, as phage samples indicated two notable size peaks, denoting vastly different diameters at substantial occurrence; a first peak at ~30 nm and the second at ~280 nm. The former size (~30 nm) is similar to that which was seen for λ*Dam15* passaged through the SupD strain in absence of plasmid. The very large error in average size determination for SupD phage preparations at this temperature can therefore likely be attributed to this bimodal size distribution.

Table 4: Sizing of λ*Dam15* phage variably decorated by gpD::eGFP

Strain [+ Plasmid] [1]	**gpD Allele**	**Times (X) increase in phage diameter** [2]			
		30ºC	**35ºC**	**37ºC**	**39ºC**
Sup⁻	gpD_{wt}	---	---	1.1 ± 0.2	---
Sup⁻ [pD::eGFP]		n/a	2.2 ± 0.5	5.5 ± 0.8	3.5 ± 0.9
SupD	gpD_{wt}	---	---	0.3 ± 0.03	---
SupD [pD::eGFP]		0.8 ± 0.1	1.2 ± 0.7	3.1 ± 1.5	1.8 ± 0.2
SupE	gpDQ68S	---	---	1.0 ± 0.1	---
SupE [pD::eGFP]		0.9 ± 0.2	1.0 ± 0.1	1.7 ± 0.2	1.2 ± 0.2
SupF	gpDQ68Y	---	---	0.67 ± 0.3	---
SupF [pD::eGFP]		1.0 ± 0.3	1.3 ± 0.2	1.6 ± 0.6	1.0 ± 0.3

[1] Lysate produced on strain at respective temp. All strains are derivatives of W3101.

[2] A minimum of three runs of triplicate determinations of size determination from DLS were divided by size determinations for naked phage grown on each of the Sup strains. Comparisons are for phage grown on SupE in absence of complementation.

[3] λ*Dam15* phage preparation on W3101 [pD] at 37ºC, expressing wild type *D* gene.

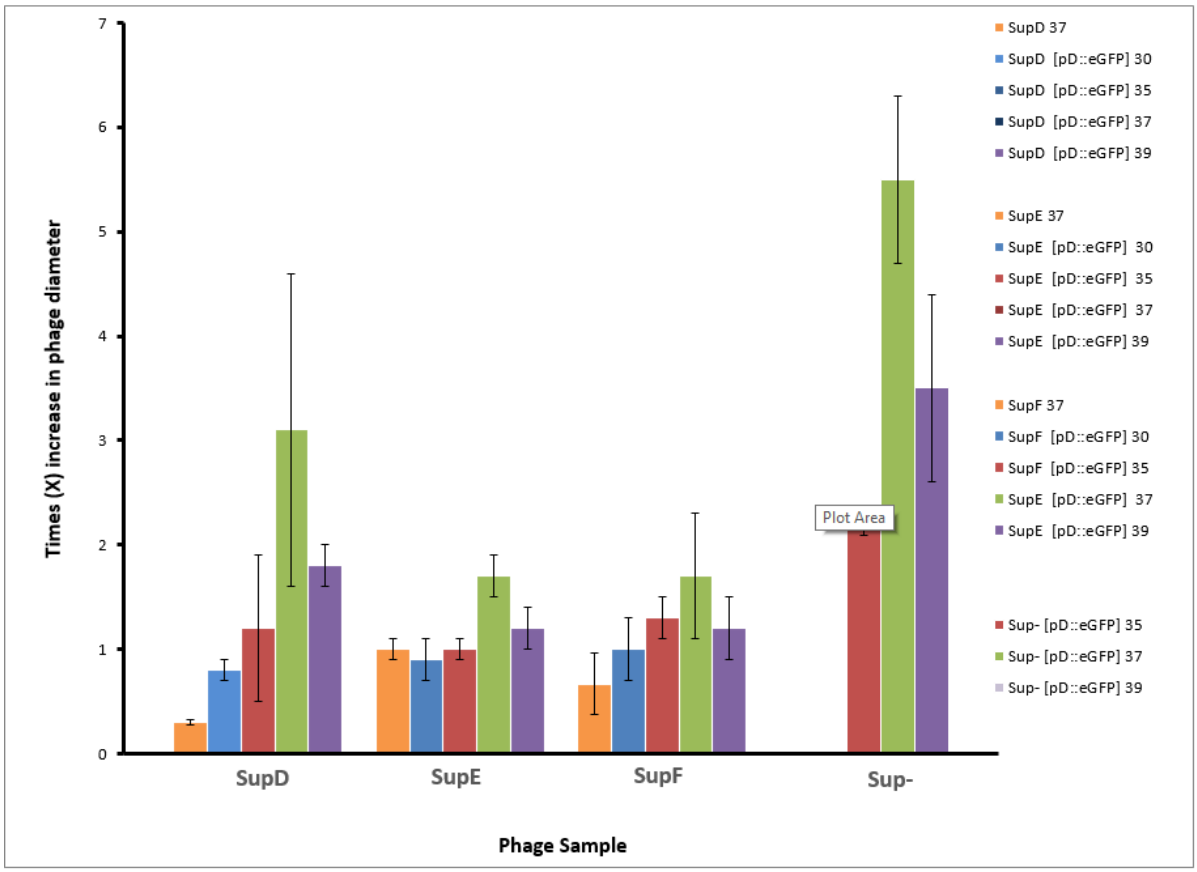

Figure 16: Sizing of λ*Dam15* phage variably decorated by gpD::eGFP. Lysates were produced on the labelled strain and at the respective temperature, standardized for titer (10^8 phage/ml), then sized by dynamic light scattering (DLS). Each size determination was repeated in triplicate. Comparisons are for phage grown on SupE (yielding gpD_{wt}) in the absence of complementation, yielding morphologically wild type λ phage that were used as the control. Each of the reported values represents the relative comparison of the experimental phage divided by the control phage size. Phage preparation on W3101 [pD] at 37°C expressing D_{wt} *in trans* are labelled in orange.

4.4 Flow cytometry of gpD::eGFP decorated phage

Lysates prepared on the Sup^+ strains at various temperatures were standardized for titer and analyzed by flow cytometry. Each sample's side scatter, which is determined mainly by the surface complexity of the phage particle, and fluorescence profile, was found to vary between phage preparations and to be influenced by the degree of gpD::eGFP capsid decoration. In collaboration with the Dr. Aucoin lab (UW, Chemical Engineering) the use of flow cytometry for this application has been previously optimized using phage passaged through SupE [pD::eGFP]. After careful deliberation and the trial of many approaches, a simple count comparison of fluorescent events was determined to be the most basic and useful analysis approach (Figure 17). An overall increase in the count of fluorescent events was observed as a function of temperature for all strains. The temperature dependence was generally more pronounced between 35^o and 37°C than between 30^o and 35°C, especially for SupD and Sup^- preparations, which can be expected since CI857 activity is exponentially diminished above 35^{o}C. For all lysate preparations, the number of fluorescent events evident was an order of magnitude higher between 35^{o}C and 37^{o}C, in agreement with the CI857 temperature-lability profile and subsequent expression of gpD::eGFP. Higher culturing temperatures corresponded well with expected higher fluorescence up to 37^{o}C due to increased gpD::eGFP expression and decoration at this temperature.

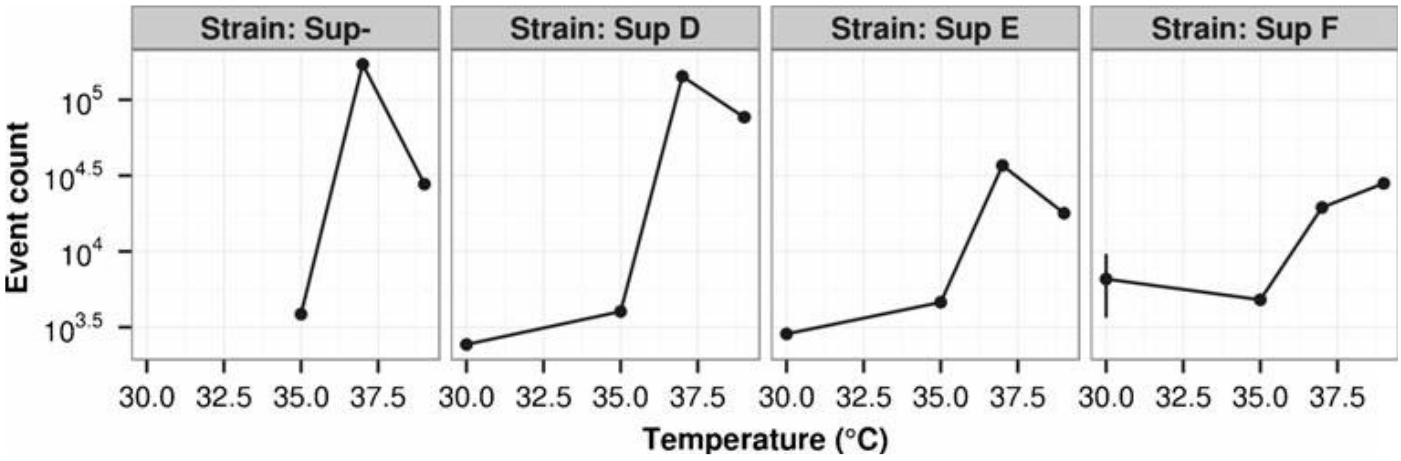

Figure 17: Mean fluorescent event counts for phage preparations on Sup—, SupD (gpDQ68S), SupE (gpD$_{wt}$) and SupF (gpDQ68Y) strains harbouring the pD::eGFP plasmid, cultured at 30º, 35º, 37º, and 39°C. Samples were standardized for titer and diluted 10-fold. Fluorescent events are those that had a fluorescence value greater than 1 (the logarithmic scale equivalent of 0). Error bars represent 95% confidence intervals around the means, calculated from triplicate measurements. In most cases, the error bars are smaller than the size of the corresponding data point. Computational and statistical analysis was performed by Stan Sokolenko as described in Sokolenko et al. (2012). Figure taken from Sokolenko et al. (2012).

Sokolenko et al. (2012) previously demonstrated that 2D fluorescence/side-scatter density is a more appropriate visualization tool for discriminating different types of fluorescent events between preparations of fluorescence-decorated λ phage. Here, we expanded on this approach to compare phage preparations on all Sup$^+$ and Sup$^-$ strains at all experimental temperatures in order to analyze all decoration permutations (Figure 18). We noted that a change in temperature from 30º to 35ºC corresponded solely to an increase in side-scatter, while an increase to 37ºC, had a greater impact on event fluorescence, as can be seen in the

prominent movement of the main cluster away from the x-axis. The low temperature changes in side-scatter can be interpreted as the result of initial capsid modification, with the increased expression of *D::eGFP* at 37ºC being required to generate a significant amount of fluorescence. Consistent with the event count analysis, strong increases in the fluorescence of λ*Dam15* lysates grown on Sup⁻ and SupD strains carrying the pD::eGFP plasmid were noted at 37ºC, as compared to the comparatively mild increase in fluorescence observed for lysates prepared on the strong suppressors, SupE and SupF. While increasing the culturing temperature to 39ºC did not significantly alter the total number of events detected, it did alter the fluorescence distribution across all preparations, most evident in the decrease of fluorescence for lysates prepared on the SupD and Sup⁻ [pD::eGFP] strains (Figure 18). The impact of increasing the expression of *D::eGFP* (by increasing the temperature beyond 37ºC on the generation of eGFP-tagged phage again appears to be limited. Similar to the results obtained for fluorimetry assays, 37ºC again was the upper limit for fluorescence, with evident reductions in fluorescence at 39-40ºC compared to that at 37ºC.

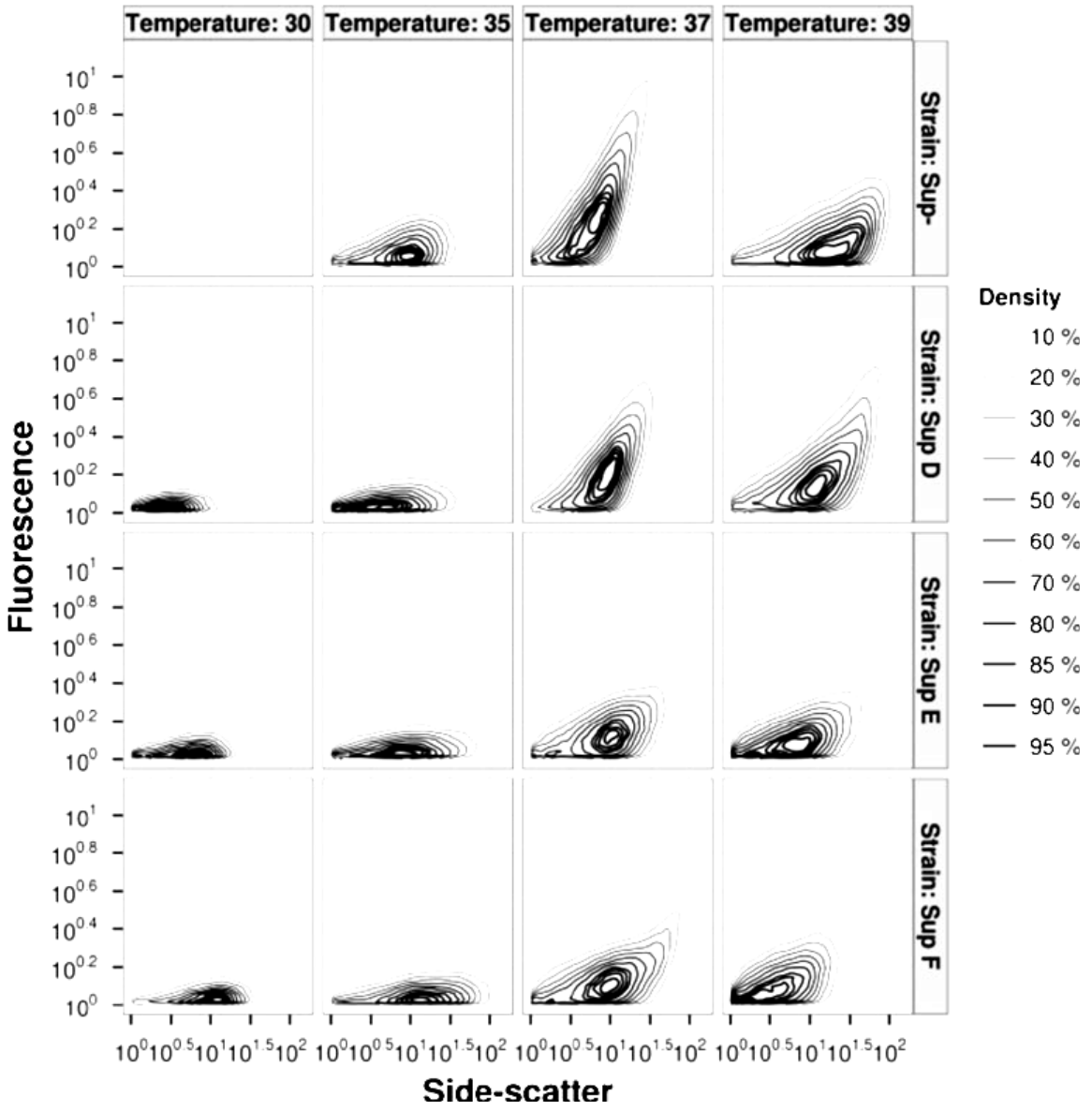

Figure 18: 2D density distribution of fluorescence vs. side scatter for phage preparations on Sup—, SupD, SupE and SupF strains carrying pD::eGFP, cultured at 30º, 35º, 37º, and 39ºC. The density distribution at each temperature is scaled to a constant height. Contour lines represent fractions of maximum density (density quantiles ranging from 0.10 to 0.95 in intervals of 0.05). Events with fluorescence or side scatter values of 1 were excluded. Samples were standardized for titer. SupD and Sup⁻ samples cultured at 37°C had high concentrations that resulted in a considerable amount of coincidence. The contours corresponding to these samples were calculated from samples diluted 10-fold with PBS; all other contours were calculated from undiluted samples to avoid excessive noise. Computational analysis of the data was performed by Stanislav Sokolenko as described in Nicastro et al. (2013).

4.5 EDTA Resistance in Decorated and Non-Decorated Phage

To assess the structural integrity of λ*Dam15* phage variably decorated by different gpD::eGFP and/or different isotypes of gpD, we next tested each of the phage samples grown at 37°C for resistance to EDTA (Table 5). EDTA or Ethylenediaminetetraacetic acid, is a chelating agent that possesses the ability to sequester divalent metal cations such as Mg^{2+}, which in turn acts to destabilize the λ phage capsid. We noted a significant variation in survival rates, whereby the lysate grown on SupE and the lysate prepared on Sup⁻[pD], both complementing the *Dam15* mutation by a gpD_{wt} allele, had the greatest EDTA resistance, with near optimal resistant progeny. Surprisingly, phage grown on SupF (gpDQ68Y), generating the gpDQ68Y allele, conferred only a 44% survival rate while those grown on SupD, generating the gpDQ68S allele, showed the poorest survival rate of 35%. The noted difference in survival rate can be attributed to the relatively stable packaging of gpD_{wt} over either of the gpDQ68Y and gpDQ68S alleles. Next, those variably decorated lysates prepared on Sup^+ [pD::eGFP] showed relatively consistent survival rates among the samples ranging from 54-59%, albeit a drop in resistance from that seen with the packaging of gpD_{wt} (SupE), and an increase in resistance from those packaging the gpDQ68Y allele (SupF) and gpDQ68S (SupD). Lysates developed on Sup⁻ [pD::eGFP] showed a relatively low survival rate of 36%. The variable display of both the fusion protein with gpD::eGFP and the gpD alleles were observably more stable than either of the gpDQ68Y, gpDQ68S or the gpD::eGFP fusion allele alone, while those incorporating gpD_{wt} were found to be the most resistant to EDTA.

Table 5: Variable susceptibility to EDTA exposure of λ*Dam15* phage

Strain [+ Plasmid] [1]	Relative efficiency of plating (EOP) [2,3]
Sup⁻ [pD]	0.93 ± 0.07
Sup⁻ [pD::eGFP]	0.36 ± 0.02
SupD [pD]-	0.35 ± 0.06
SupD [pD::eGFP]	0.59 ± 0.02
SupE [pD]-	0.91 ± 0.04
SupE [pD::eGFP]	0.54 ± 0.02
SupF [pD]-	0.44 ± 0.02
SupF [pD::eGFP]	0.57 ± 0.07

[1] Lysate produced on strain at 37°C. All strains are derivatives of W3101.

[2] Calculated from a minimum of three determinations, grown on BB4 (*SupE, SupF*).

[3] All EOP determinations were determined from a minimum of three assays and using the original universal determined concentration of 4 X 10^8 grown on BB4 (*SupE, SupF*) as the positive (100%) plating control.

4.6 Relationship between Fluorescence and Size of Decorated Phage Preparations

A plot was developed to assess the relationship between the fluorescence and size ratios of decorated and non-decorated phage (Figure 19). All phage samples were compared to the size of the undecorated control phage grown on SupE (gpD_{wt}) in the absence of pD::eGFP. Undecorated negative controls were used as the base size for each sample batch. These samples were grown on Sup^+ strains permitting the incorporation of respective wild-type length gpD alleles. Each series was plotted as a separate plot to best emphasize the relationship from each individual negative control. We noted a relationship between the decoration and size of phage whereby an increase to the number of decorated phage head particles saw a comparative increase to the phage head size in comparison to phage which only harbored the wild-type length alleles. This would be indicative of an increase to phage head complexity as previously mentioned (sections 4.2 and 4.3) as well as an overall change to the phage capsid diameter upon addition of the decorated fusions.

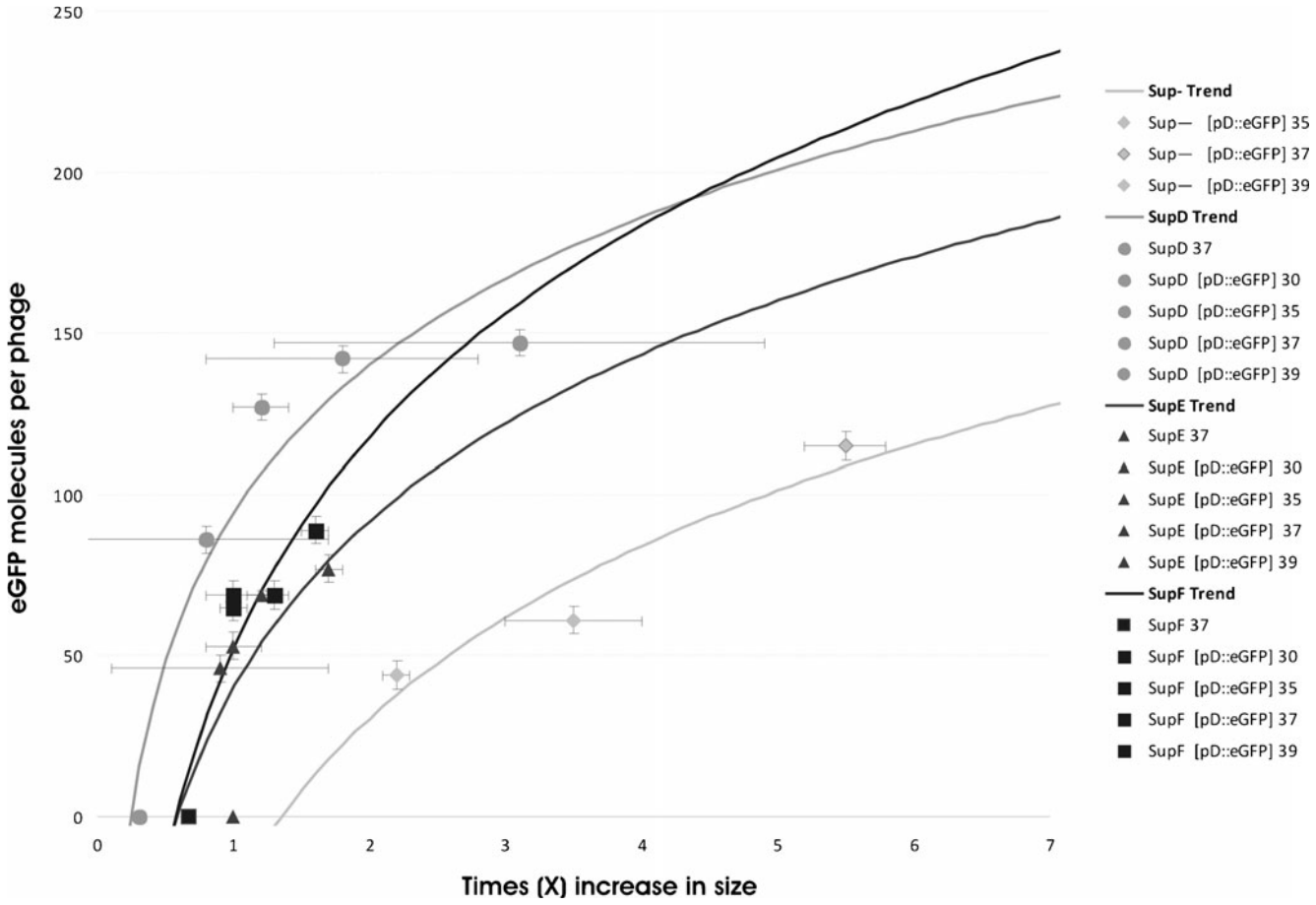

Figure 19: Separation of decorated phage preparations based on fluorescence emitted and size as determined by dynamic light scattering. Fluorescence and size ratios based on comparison to λ*Dam15* grown on W3101 SupE (gpD_{wt}) in the absence of a pD::eGFP plasmid. The measured sizes are reported using a percent intensity distribution. Each data point was automatically repeated in triplicate, and the average is reported. Sizing results are expressed based on "X" increase compared to λ*Dam15* grown on the BB4 providing gpD_{wt} and gpDQ68Y incorporation into the resultant phage capsid. Measured fluorescence data was analyzed by Stanislav Stokolenko using the SoftMaxPro V5 software based on 6 readings and the samples were run in duplicate with the average being reported. Phage samples were run alongside an eGFP standard to determine the protein concentrations of each sample. The determined eGFP molecules per phage was interpolated through Excel against a derived equation of the trend-line from known eGFP purified protein fluorescence calibration curve and the weight of the eGFP molecule. Figure taken from Nicastro et al. (2013)

5 Discussion

Maruyama et al. (1994) and Mikawa et al. (1996) first modulated total fusion protein incorporated on the capsid through the use of amber stop codons, located upstream of the *V D* genetic fusion. As such, the level of decoration was dependent on the strength of suppression supplied by the host bacterial Sup^+ mutant through which the phage was passaged. These initial studies provided a great foundation and premise for this work while also providing preliminary insight into some of the challenges that would be faced and complications to be overcome. Here, we sought to design and characterize a phage display platform to more finely control decoration of gpD fusions on the surface of λ phage, using eGFP as the fusion partner. This combines two competing genetic principles: 1) Generation of different alleles of gpD with different structural functionality suppressing the λ*Dam15* mutation; and 2) plasmid-borne *D::X* fusion expression regulated by temperature to complement the *Dam15* mutation. We have shown here that through the combination of these two dimensions a wide breadth of permutations in phage decoration through gpD::X fusions can be achieved.

The gpD::eGFP C-terminal fusion was able to complement and restore viability to the λ*Dam15* phage, but despite the presence of the linker, the fusion was found to reduce functionality of the major capsid protein marginally in the Sup^- host, compared to its unfused counterpart, which is likely due to the size of the fusion generated. Previously, Yang et al. (2000) noted that the presence of a large protein fusion disrupts phage assembly due to

the overloading of recombinant protein that decreases phage viability. Vaccaro et al. (2006) later reported that fusion of a scFv sequence to the C-terminal of gpD employing a double gene *D* system and a flexible linker between the fusion peptide and gpD similarly resulted in smaller plaque size and reduced phage viability.

The exact positioning of the λF7 (λ*Dam15imm21ts*) mutation was previously determined in our lab (Nicastro et al. 2013, Sheldon 2013) after sequencing of the 333 bp *Dam15* allele to find that the amber mutation was localized to the 204th bp of *D*. This transition imparts the conversion of the 68th CAG codon (glutamine), to an amber translational stop signal (UAG) codon. In a Sup^{-} host the amber mutation imparts a premature translational stop resulting in a truncated 68 a.a. non-functional gpD fragment that is incapable of stabilizing and packaging full length λ DNA. Growing λ *Dam15* phage on an amber suppressor host may result in a phenotypic a.a. substitution of glutamine residue at position 68. Only a SupE strain will code glutamine at the 68th codon restoring the pristine sequence of gpD, while SupD will confer a serine substitution, producing a gpDQ68S; and SupF will confer a tyrosine substitution, yielding gpDQ68Y.

In this study, the assembly of viable phage depended on the tolerance of the λ phage capsid for the gpD allele conferred by each of the suppressor strains, in addition to that of the gpD::eGFP fusions. While restoration of the pristine sequence (in SupE) was expected to restore full function to gpD, it was somewhat surprising that the substitution of the glutamine, a carboxamide, 146.2 Da, polar neutral a.a. with tyrosine, a bulky (181.2 Da), aromatic and hydrophobic a.a. restored nearly full viability to the λ*Dam15* phage. Lastly, the substitution of glutamine with the albeit smaller (105.1 Da) serine (gpDQ68S) that is

biochemically similar as a polar neutral a.a., provided very little improvement compared to that on the Sup⁻ (gpD⁻) in restoring viability to λ *Dam15,* and generated comparatively very small phage and pinpoint plaques in the absence of gpD or gpD::eGFP complementation. Possible reasons for the dramatic effect of the serine substitution at residue 68 of gpD (Nicastro et al. 2013, Sheldon 2013) include interference in gpD trimerization and/or compromised interaction with gpE hexamers, although previous findings indicate that the N-terminus is located closer to the 3-fold axis of the gpD trimer (Yang et al. 2000) and may be involved with interacting with gpE. The functionality of gpD derivatives was similarly reflected in phage sizing of undecorated phage. SupD phage preparations carrying the gpDQ68S allele were only a third the size of wild type (SupE) and SupF preparations. While SupE and SupF host progeny likely possessed close to a full complement (405-420) of gpD per capsid, SupD phage progeny instability is likely due to being minimally decorated. To assess stability, we examined EDTA resistance of various preparations in presence and absence of *D::eGFP* expression and found that phages carrying the gpDQ68S protein were the most unstable. The instability of phage yielded from these preparations explains the large variation in eGFP per phage and sizing found for this group, whereby these phage are likely prone to capsid disassembly. This instability was similarly found for phage assembled in the presence of the fusion alone; again indicating that stability necessitates the capsid incorporation of gpD in order to stabilize fusion decoration.

Despite the potential 405 to 420 gpD incorporations into the phage capsid, our results suggest that the highest incorporation possible using our system was only 147 gpD::eGFP molecules/phage. Even in the absence of gpD (on Sup⁻) the incorporation of gpD::eGFP was

restricted to 115 molecules per phage, indicating that a full complement of gpD is not necessary to restore viability to λ*Dam15* and that in the absence of a wild type or gpD derivative, fusion incorporation into the phage is limited. Mikawa et al. (1996) previously reported that a scenario where all gpD sites on the capsid were occupied by C-terminal gpD fusion proteins was not achievable, as resultant phage were still sensitive to EDTA, indicative of empty gpD sites. Similarly, in this study, phage samples prepared at 35˚C were found to complement for viability reasonably well despite the relatively low levels of gpD::eGFP incorporation, which was only source of gpD in this preparation. These samples were found to only harbour 44 gpD::eGFP molecules/phage (~10% of available gpD capsid sites), which was corroborated by a smaller reported average phage diameter.

Mikawa et al. (1996) showed that plasmid copy number does affect the level of expression and therefore ability to complement for a *D* mutation (Mikawa et al. 1996; Sternberg and Hoess 1995). In this work, plasmid copy number was not used as an approach to control decoration and a multicopy plasmid was employed for all constructs, but this may be of interest in future studies where multiple fusions could be incorporated simultaneously into a phage capsid. The manipulation of plasmid copy number could provide a third dimension of control. Zucconi *et* al. (2001) and Minenkova et al. (2003) also found that the number of fusion proteins displayed on the λ capsid surface varied depending on the length and a.a. composition of the foreign sequence expressed at the C-terminal of gpD. Santini et al. (1998) also observed a similar result where fusion of large protein domains to gpD significantly reduced the titer of phage when grown on Sup^{-} compared to Sup^{+} strains. This finding indicated that incorporating wild-type D protein is preferential for proper assembly, and that

the use of suppressor strains is advantageous (Santini et al. 1998). Similarly, Yang et al. (2000) also reported that the interference in phage assembly they noted by overloading the phage with fusion protein was not observed in previous studies where recombinant protein was incorporated with wild-type gpD, again suggesting the role of wild type gpD in improving incorporation of the fusion (Yang et al. 2000).

While suppression correlated well to restoration of phage viability, the opposite was true when we examined fluorescence of the various phage preparations in the presence of *D::eGFP* expression. Phage prepared on the best suppressors showed low fluorescence even under conditions of high gpD::eGFP production, while the SupD suppressor offered the highest levels of eGFP phage decoration, even under conditions where *D::eGFP* expression was only leaky (30^{o}C). Previous studies similarly reported that low yields and decreased phage viability are associated with greater expression of capsid-fusion protein, although at the time it was not clear whether this observation was due to impaired capsid assembly (Mikawa et al. 1996; Maruyama et al. 1994).

We attribute this finding to the accumulation of gpD derivatives, or intragenically complementary heterotrimers with higher functionality into the capsid, thereby reducing the incorporation of the less preferred allele or homo/heterotrimer combinations. In the case of SupE and SupF host preparations, the full length gpD alleles were preferred over the gpD::eGFP fusion even at high levels of expression, thereby reducing fluorescence to the resultant phage. In contrast, in SupD preparations, the preferred allele may be gpD::eGFP that "outcompetes" the gpDQ68S allele for placement into the capsid, resulting in stronger decoration. These inferences are supported by phage sizing data, which demonstrate a

positive correlation between fluorescence and size of the resultant phage particles (Figure 1). This data supports the assumption that the amount of eGFP fusions on the phage surface can be quantified through florescent measurements and that with an increase in gpD::eGFP fusions, a proportional increase in the phage diameter would be expected. This data was similarly demonstrated by cytometry analysis of fluorescence and side scatter. Here, the 2D fluorescence/side-scatter density distribution (Figure 18) corroborated fusion decoration trends and as previously suggested (Sokolenko et al. 2012), indicated increasing side scatter alongside heightened fluorescence (eGFP decoration), relating phage surface complexity to degree of capsid fusion incorporation.

While the eGFP phage decoration profile fits well for increasing *D::eGFP* derepression from 30^{o} through 37^{o}C, at the highest level of fusion expression from λ *pL* (39–40^{o}C), where CI857 repressor is completely labile, gpD::eGFP phage decoration decreases compared to that at 37^{o}C on all host cell line preparations. We attribute this finding to the mode of lysate preparation that exposes host cells to heat-shock temperatures for several hours, altering cell physiology and increasing concentration of heat shock response proteins (Hsp) factor (Gill et al. 2000, Smith 2007, Valdez-Cruz et al. 2010). This response includes the up-regulation of genes coding for heat shock proteins and SOS response, with the particular attention to proteases such as *clpP*, *degP*, *ftsH*, *ompT* and *lon*, regulated by the σ^{32} sigma factor. Temperature inducing up-shifts impart high physiological stress to the host cell that results in a three-fold increase in global protein synthesis, a quarter of which is devoted to Hsp synthesis (G. Wegrzyn and Wegrzyn 2002; Hoffmann and Ursula Rinas 2001; Zhao et al. 2005; Yamamori and Yura 1980; Hoffmann and Rinas 2000; Valdez-Cruz et al. 2010),

thereby reducing growth rates and recombinant protein yield (Wegrzyn and. Wegrzyn 2002; Valdez-Cruz et al. 2010; Zhao et al. 2005). Also, recombinant proteins produced using thermoinduction systems, particularly from multicopy plasmids as in this work, can result in high protein concentrations and the formation of inclusion bodies, removing these proteins from the functional fusion population (Babu et al. 2000; Rinas and Hoffmann 2004; Caspeta et al. 2009; Vallejo et al. 2002; Valdez-Cruz et al. 2010).

The potential downstream applications of this research are primarily the construction of multivalent phage vaccines and/or the development of vehicles for phage-mediated targeted gene therapy. These applications exhibit the two endpoints of the spectrum of phage surface display control. While vaccination would expectedly be most effective if display saturation was reached, targeted transgene delivery applications would require a high-level of specificity in targeting unique receptors of appropriate cells, where fewer and controlled fusions are usually preferable. It is important to note that while our system demonstrates a fair degree of variability in eGFP decoration, these results are only useful in relative comparison of phage decoration conditions. Absolute display will be dependent upon the size and biochemical attributes of the fused candidate and the tolerance of gpD and the foreign polypeptide to fusion.

Chapter 6: Conclusion

The intention of this work is to develop a phage display platform that permits the stable and highly-controllable phage display *via* two-dimensional genetic control over the co-expression of gpD alleles and a gpD::eGFP fusion protein on temperate bacteriophage λ. This system utilizes the bacteriophage λ capsid protein gpD for the fusion of eGFP polypeptides for the efficient display on the surface of the phage. Amber suppression control was established through the use of gpD alleles generated during λ *Dam15* infection of Sup^+ isogenic derivatives. These particles carry gpD alleles of varying functionality depending on the amber suppressor strain of *E. coli*, SupD (gpDQ68S), SupE (D_{wt}) or SupF (gpDQ68Y) host on which they were grown. In combination, temperature control was employed through the use of the D-fusion protein, gpD::eGFP, encoded *in trans* from a multicopy temperature-inducible expression plasmid regulated by the λ CI857 repressor. This combinational control system generated dramatic variation in the expression of displayed peptides through the many permutations afforded by the dual mechanisms of control. Maximal incorporation of gpD::eGFP into the λ*Dam15* phage capsid was imparted in combination with the gpDQ68S allele, despite the fact that SupD proved to be the worst suppressor of the *Dam15* mutation. Temperature-regulated *D::eGFP* fusion expression from the pD::eGFP plasmid in combination with functional breadth of gpD alleles afforded by variable suppression of *Dam15* conferred resultant phage that differed in size, fluorescence and absolute protein decoration (Nicastro et al. 2013, Sokolenko et al. 2012).

Phage display offers many important applications to date and a fine-tuned system as mentioned in this work could significantly improve future applications by tailoring decoration to the needs of the application at hand. The industrial use of phage display has been increasing in interest. Although the applications have been significant, the use of phage display in industry has seen primarily horizontal growth, where the system has remained virtually identical, but the number of applications has been increasing. With respect to clinical applications, the two-gene system has empowered phage display in therapeutic design; however, control of the fusion copy number is highly necessary but has to date proven a formidable obstacle. For example, phage vaccines need maximal expression of the target antigen to induce a strong response (Hayes et al. 2010), which can be an issue with the two gene-systems, since they will normally result in a greater number of wild-type protein (Enshell-Seijffers et al. 2001). Mammalian gene delivery systems also require control of copy number such that the phage vectors display a combination of peptides (Lankes et al. 2007). The incorporation of control over fusion decoration is critical to the efficacy of phage-based biotherapeutics and the work described here makes strong inroads into addressing this issue.

Future research objectives:

1) Continued and completed analysis testing the expression at the carboxy terminal of the *D::gfp* fusion on the amber suppressor strains with the plasmid for the incorporation of D::eGFP under the control of a temperature *cI857* sensitive repressor.

2) Exploitation of the system to clinically relevant peptides and fusions including those for vaccine delivery and the development of a universal antimicrobial.

3) Construction of a system that is transferrable to N15 and create N, C and N+C terminal fusions with gp7

4) TEM (Transmission Electron microscope) imaging of the displayed peptides

References

Aucoin, M. G., McMurray-Beaulieu, V., Poulin, F., Boivin, E. B., Chen, J., Ardelean, F. M., Cloutier, M., Choi Y.J., Miguez, C.B., & Jolicoeur, M. (2006). Identifying conditions for inducible protein production in *E. coli:* combining a fed-batch and multiple induction approach. *Microbial Cell Factories, 5*, 27.

Babu, K. R., Swaminathan, S., Marten, S., Khanna, N., & Rinas, U. (2000). Production of interferon-a in high cell density cultures of recombinant *Escherichia coli* and its single step purification from refolded inclusion body proteins. *Applied Microbiology and Biotechnology*, *53*, 655–660.

Bachmann, B. J. (1972). Pedigrees of some mutant strains of *Escherichia coli* K-12. *Microbiology and Molecular Biology Reviews : MMBR*, *36*(4), 525–557.

Barry, M., Dower, W., & Johnston, S. A. (1996). Toward cell-tergetting gene therapy vectors: selection of cell-binding peptides from random peptide-presenting phage libraries. *Nature Medicine*, *2*(3), 299–305.

Bastien, N., Trudel, M., & Simard, C. (1997). Protective immune responses induced by the immunization of mice with a recombinant bacteriophage displaying an epitope of the human respiratory syncytial virus. *Virology*, *234*(1), 118–122.

Beghetto, E., & Gargano, N. (2011). Lambda-display: a powerful tool for antigen discovery. *Molecules (Basel, Switzerland)*, *16*(4), 3089–3105.

Benzer, S., & Champe, S. P. (2013). A change from nonsense to sense in the genetic code. *Proceedings of the National Academy of Sciences of the United States of America*, *48*(7), 1114–1121.

Bernard, H., Remaut, E., Hershfield, M., Das, H., Helinski, D., Yanofsky, C., & Franklin, N. (1979). Construction of plasmid cloning vehicles that promote gene expression from the bacteriophage lambda pL promoter. *Gene*, *5*, 59–76.

Breitling, R., Sorokin, A., & Behnke, D. (1990). Temperature-inducible gene expression in *Bacillus subtillis* mediated by the cI857-encoded repressor of bacteriophage lambda. *Gene*, *93*, 35–40.

Brigati, J., Williams, D. D., Sorokulova, I. B., Nanduri, V., Chen, I.-H., Turnbough, C. L., & Petrenko, V. A. (2004). Diagnostic probes for *Bacillus anthracis* spores selected from a landscape phage library. *Clinical Chemistry*, *50*(10), 1899–906.

Caspeta, L., Flores, N., Pérez, N. O., Bolívar, F., & Ramírez, O. T. (2009). The effect of heating rate on *Escherichia coli* metabolism, physiological stress, transcriptional response, and production of temperature-induced recombinant protein: a scale-down study. *Biotechnology and Bioengineering*, *102*(2), 468–482.

Clark, J. R., Bartley, K., Jepson, C. D., Craik, V., & March, J. B. (2011). Comparison of a bacteriophage-delivered DNA vaccine and a commercially available recombinant protein vaccine against hepatitis B. *FEMS Immunology and Medical Microbiology*, *61*(2), 197–204.

Clark, J. R., & March, J. B. (2004). Bacteriophage-mediated nucleic acid immunisation. *FEMS Immunology and Medical Microbiology*, *40*, 21–26.

Clark, J. R., & March, J. B. (2006). Bacteriophages and biotechnology: vaccines, gene therapy and antibacterials. *Trends in Biotechnology*, *24*(5), 212–218.

d'Herelle, F., & Smith, G. . (1926). *The bacteriophage and its behavior* (pp. 413–424). Baltimore, MD: The Williams & Wilkins Company.

Dabrowska, K., Opolski, A., & Gorski, A. (2005). Bacteriophage penetration in vertebrates. *Journal of Applied Microbiology*, *98*, 7–13.

Dai, M., Temirov, J., Pesavento, E., Kiss, C., Velappan, N., Pavlik, P., Werner, J.H., & Bradbury, A. R. M. (2008). Using T7 phage display to select GFP-based binders. *Protein Engineering, Design & Selection : PEDS*, *21*(7), 413–424.

Dickerson, T. J., Kaufmann, G. F., & Janda, K. D. (2005). Bacteriophage-mediated protein delivery into the central nervous system and its application in immunopharmacotherapy. *Peptides, Proteins and Antisense*, *5*(6), 773–781.

Dokland,T., Murialdo, H. (1993). Structrual transitions during maturation of bacteriophage lambda Capsids. *Journal of Molecular Biology*, *233*, 682–694.

Duckworth, D. H. (1976). Who discovered bacteriophage? *Bacteriological Reviews*, *40*(4), 793–802.

Dulbecco, R. (1982). Viruses with recombinant surface proteins. United States of America.

Dunn, I. S. (1995). Assembly of functional bacteriophage lambda virions incorporating C-terminal peptide or protein fusions with the major tail protein. *Journal of Molecular Biology*, *248*(3), 497–506.

Dunn, I. S. (1996). Mammalian cell binding and transfection mediated by surface-modified bacteriophage lambda. *Biochimie*, *137*(1838), 37.

Efimov, V. P., Nepluev, I. V, & Mesyanzhinov, V. V. (1995). Bacteriophage T4 as a surface display vector. *Virus Genes*, *10*(2), 173–177.

Eggertsson, G., & Söll, D. (1988). Transfer ribonucleic acid-mediated suppression of termination codons in *Escherichia coli*. *Microbiological Reviews*, *52*(3), 354–374.

Eguchi, A., Akuta, T., Okuyama, H., Senda, T., Yokoi, H., Inokuchi, H., … Nakanishi, M. (2001). Protein transduction domain of HIV-1 Tat protein promotes efficient delivery of DNA into mammalian cells. *The Journal of Biological Chemistry*, *276*(28), 26204–26210.

Enshell-Seijffers, D., Smelyanski, L., & Gershoni, J. M. (2001). The rational design of a "type 88" genetically stable peptide display vector in the filamentous bacteriophage fd. *Nucleic Acids Research*, *29*(10), 50–60.

Fischetti, V. a. (2005). Bacteriophage lytic enzymes: novel anti-infectives. *Trends in Microbiology*, *13*(10), 491–496.

Funatsu, T., Taniyama, T., Tajima, T., Tadakuma, H., & Namiki, H. (2002). Rapid and sensitive detection method of a bacterium by using a GFP reporter phage. *Microbiology and Immunology*, *46*(6), 365–369.

Gamage, L. N. a, Ellis, J., & Hayes, S. (2009). Immunogenicity of bacteriophage lambda particles displaying porcine Circovirus 2 (PCV2) capsid protein epitopes. *Vaccine*, *27*(47), 6595–6604.

Garufi, G., Minenkova, O., Lo Passo, C., Pernice, I., & Felici, F. (2005). Display libraries on bacteriophage lambda capsid. *Biotechnology Annual Review*, *11*, 153–190.

Georgopoulos, C., Tilly, K., & Casjens, S. (1983). Lambdoid phage head assembly. In R. Hendrix, J. W. Roberts, F. Stahl, & R. Weisberg (Eds.), *Lambda II* (pp. 279–304). Cold Springs Harbor, New York: Cold Spring Harbor Laboratory.

Gill, R. T., Valdes, J. J., & Bentley, W. E. (2000). A comparative study of global stress gene regulation in response to overexpression of recombinant proteins in *Escherichia coli*. *Metabolic Engineering*, *2*(3), 178–189.

Gulig, P., Martin, J., Messer, H. G., Deffense, B. L., & Harpley, C. J. (2008). Phage display methods for detection of bacterial pathogens. In M. Zourpb, S. Elwary, & A. Turner (Eds.), *Principles of Bacterial Detection: Biosensors, Regognition Receptors and Microsystems* (pp. 755–783). Montreal, Canada: Springer.

Gupta, A., Onda, M., Pastan, I., Adhya, S., & Chaudhary, V. K. (2003). High-density Functional Display of Proteins on Bacteriophage Lambda. *Journal of Molecular Biology*, *334*(2), 241–254.

Guzmán, C. A., Piatti, G., Walker, M. J., Guardati, M. C., & Pruzzo, C. (1994). A novel *Escherichia coli* expression-export vector containing alkaline phosphatase as an insertional inactivation screening system. *Gene*, *148*(1), 171–172.

Haq, I. U., Chaudhry, W. N., Akhtar, M. N., Andleeb, S., & Qadri, I. (2012). Bacteriophages and their implications on future biotechnology: a review. *Virology Journal*, *9*(1), 9.

Hart, S. L., Knight, a M., Harbottle, R. P., Mistry, A., Hunger, H. D., Cutler, D. F., Williamson, R., Coutelle, C. (1994). Cell binding and internalization by filamentous phage displaying a cyclic Arg-Gly-Asp-containing peptide. *The Journal of Biological Chemistry*, *269*(17), 12468–74.

Hayes, S., Gamage, L. N. a, & Hayes, C. (2010). Dual expression system for assembling phage lambda display particle (LDP) vaccine to porcine Circovirus 2 (PCV2). *Vaccine*, *28*(41), 6789–6799.

Hayes, S., & Hayes, C. (1986). Spontaneous lambda OR mutations suppress inhibition of bacteriophage growth by nonimmune exclusion phenotype of defective lambda prophage. *Journal of Virology*, *58*(3), 835–842.

Hoffmann, F., & Rinas, U. (2000). Kinetics of heat-shock response and inclusion body formation during temperature-induced production of basic fibroblast growth factor in

high-cell-density cultures of recombinant *Escherichia coli*. *Biotechnology Progress*, *16*(6), 1000–1007.

Hoffmann, F., & Rinas, U. (2001). On-line estimation of the metabolic burden resulting from the Synthesis of Plasmid-Encoded and Heat-Shock proteins by monitoring respiratory energy Generation. *Biotechnology and Bioengineering*, *76*(4), 333–340.

Hohn, T., & Katsura, I. (1977). Structure and assembly of bacteriophage lambda. In W. Arber, W. Henle, P. H. Hofschneider, J. H. Humphrey, J. Klein, P. Koldovský, H. Koprowski, O. Maaløe, F. Melchers, R. Rott, H.G. Schweiger, I. Syruček, Vogt, P K P. K. Vogt (Eds.), *Current Topics in Microbiology and Immunology SE - 3* (Vol. 78, pp. 69–110). Springer Berlin Heidelberg.

Ide, T., Bik, S., Matsuba, T., & Marayama, S. H. (2003). Identifcation by the phage-display technique of peptides that bind to H7 flagellin of *Escherichia coli*. *Bioscience, Biotechnology, and Biochemistry*, *67*(6), 1335–1341.

Inokuchi, H., Yamao, F., Sakano, H., & Ozeki, H. (1979). Identification of transfer RNA suppressors in *Escherichia coli*. *Journal of Molecular Biology*, *132*, 649–662.

Jacob, F., & Wollman, É. L. (1961). *Sexulality and Genetics of Bacteria* (pp. 1–374). New York: Academic Press.

Jechlinger, W., Szostak, M. P., Witte, A., & Lubitz, W. (1999). Altered temperature induction sensitivity of the lambda pR/cI857 system for controlled gene E expression in *Escherichia coli*. *FEMS Microbiology Letters*, *173*(2), 347–352.

Jepson, C. D., & March, J. B. (2004). Bacteriophage lambda is a highly stable DNA vaccine delivery vehicle. *Vaccine*, *22*(19), 2413–2419.

Jestin, J.-L. (2008). Functional cloning by phage display. *Biochimie*, *90*(9), 1273–1278.

Kaiser, A. D. . (1966). On the internal structure of bacteriophage lambda. *The Journal of General Physiology*, *49*(6), 171–178.

Kalniņa, Z., Siliņa, K., Meistere, I., Zayakin, P., Rivosh, A., Abols, A., Leja, M., Minenkova, O., Schandendorf, D., & Linē, A. (2008). Evaluation of T7 and lambda phage display systems for survey of autoantibody profiles in cancer patients. *Journal of Immunological Methods*, *334*(1-2), 37–50.

Katsura, I. (1983). Tail Assembly and Injection. In R. Hendrix, J. Roberts, F. Stahl, & R. Weisberg (Eds.), *Lambda II* (pp. 331–346). Cold Springs Harbor, New York: Cold Spring Harbor Laboratory.

Kehoe, J. W., & Kay, B. K. (2005). Filamentous phage display in the new millennium. *Chemical Reviews*, *105*, 4056–4072.

Lander, G. C., Evilevitch, A., Jeembaeva, M., Potter, C. S., & Johnson, J. E. (2008). Bacteriophage lambda stabilization by auxiliary protein gpD: timing, location, and mechanism of attachment determined by cryoEM. *Structure*, *16*(9), 1399–1406.

Lankes, H. a, Zanghi, C. N., Santos, K., Capella, C., Duke, C. M. P., & Dewhurst, S. (2007). In vivo gene delivery and expression by bacteriophage lambda vectors. *Journal of Applied Microbiology*, *102*(5), 1337–1349.

Larocca, D., & Baird, A. (2001). Receptor-mediated gene transfer by phage-display vectors: applications in functional genomics and gene therapy. *Drug Discovery Today*, *6*(15), 793–801.

Letelier, L., Plancon, L., & Boulanger, P. (2007). Transfer of DNA from Phage to Host. In S. Mc Grath & D. van Sinderen (Eds.), *Bacteriophage: Genetics and Molecular Biology* (pp. 1–357). Caister Academic Press.

Li, P., Yu, L., Wu, X., Bai, W., Li, K., Wang, H., Hu, G., Zhang, L., Zhang, F., & Xu, Z. (2012). Modification of the adenoviral transfer vector enhances expression of the Hantavirus fusion protein GnS0.7 and induces a strong immune response in C57BL/6 mice. *Journal of Virological Methods*, *179*(1), 90–96.

Lieb, M. (1966). Studies of heat-inducible lambda bacteriophage. *Journal of Molecular Biology*, *16*(1), 149–163.

Lindqvist, B. (2005). *Phage in Display* (Second Edi., pp. 686–694). Oxford University Press.

Ling, Y., Liu, W., Clark, J. R., March, J. B., Yang, J., & He, C. (2011). Veterinary Immunology and Immunopathology Protection of mice against Chlamydophila abortus infection with a bacteriophage-mediated DNA vaccine expressing the major outer membrane protein. *Veterinary Immunology and Immunopathology*, *144*(3-4), 389–395.

Loessner, M. J., Rudolf, M., Scherer, S., & Icrobiol, A. P. P. L. E. N. M. (1997). Evaluation of luciferase reporter bacteriophage A511 :: luxAB for detection of *Listeria monocytogenes* in contaminated foods. *Microbiology*, *63*(8), 2961–2965.

Lowman, H. B., & Bina, M. (1990). Temperature-mediated regulation and downstream inducible selection for controlling gene expression from the bacteriophage lambda pL promoter. *Gene*, *96*(1), 133–136.

Lukacik, P., Barnard, T. J., Keller, P. W., Chaturvedi, K. S., Seddiki, N., Fairman, J. W., Noinaj, N., Kirby, T.L., Henderson, J.P., Steven, A.C., Hinnebusch, B.J. & Buchanan, S. K. (2012). Structural engineering of a phage lysin that targets gram-negative pathogens. *Proceedings of the National Academy of Sciences of the United States of America*, *109*(25), 9857–9862.

Malanchère-Brès, E., Payette, P. J., Mancini, M., Tiollais, P., Davis, L., & Michel, M. (2001). CpG oligodeoxynucleotides with hepatitis B surface antigen (HBsAg) for vaccination in HBsAg-transgenic mice. *Journal of Virology*, *75*(14), 6482–6491.

March, J. B., Clark, J. R., & Jepson, C. D. (2004). Genetic immunisation against hepatitis B using whole bacteriophage lambda particles. *Vaccine*, *22*, 16666–1671.

Maruyama, I. N., Maruyama, H. I., & Brenner, S. (1994). Lambda foo: a lambda phage vector for the expression of foreign proteins. *Proceedings of the National Academy of Sciences of the United States of America*, *91*(17), 8273–8277.

Mattiacio, J., Walter, S., Brewer, M., Domm, W., Friedman, A. E., & Dewhurst, S. (2011). Dense display of HIV-1 envelope spikes on the lambda phage scaffold does not result in the generation of improved antibody responses to HIV-1 Env. *Vaccine*, *29*(14), 2637–2647.

Mikawa, Y. G., Maruyama, I. N., & Brenner, S. (1996). Surface display of proteins on bacteriophage lambda heads. *Journal of Molecular Biology*, *262*(1), 21–30.

Min, J.-J., Nguyen, V. H., & Gambhir, S. S. (2010). Molecular imaging of biological gene delivery vehicles for targeted cancer therapy: beyond viral vectors. *Nuclear Medicine and Molecular Imaging*, *44*(1), 15–24.

Minenkova, O., Pucci, A., Pavoni, E., De Tomassi, A., Fortugno, P., Gargano, N., Cianfriglia, M., Barca, S., De Placido, S., Martignetti, A., Felici, F., Cortese, R., Monaci, P. (2003). Identification of tumor-associated antigens by screening phage-displayed human cDNA libraries with sera from tumor patients. *International Journal of Cancer. Journal International Du Cancer*, *106*(4), 534–544.

Mott, J. E., Grant, R. a, Ho, Y. S., & Platt, T. (1985). Maximizing gene expression from plasmid vectors containing the lambda PL promoter: strategies for overproducing transcription termination factor rho. *Proceedings of the American Thoracic Society*, *82*(1), 88–92.

Mullen, L. M., Nair, S. P., Ward, J. M., Rycroft, A. N., & Henderson, B. (2006). Phage display in the study of infectious diseases. *Trends in Microbiology*, *14*(3), 141–147.

Nakanishi, M., Eguchi, A., Akuta, T., Nagoshi, E., Fujita, S., Okabe, J., … Hasegawa, M. (2003). Basic peptides as functional components of non-viral gene transfer vehicles. *Current Protein and Peptide Science*, *4*(2), 141–150.

Nicastro, J., Sheldon, K., El-Zarkout, F. a, Sokolenko, S., Aucoin, M. G., & Slavcev, R. (2013). Construction and analysis of a genetically tuneable lytic phage display system. *Applied Microbiology and Biotechnology*, *97*(17), 7791–7804.

Nicastro, J., Sheldon, K., & Slavcev, R. a. (2014). Bacteriophage lambda display systems: developments and applications. *Applied Microbiology and Biotechnology*, *98*(7), 2853–2856.

Normanly, J., Massont, J., Kleinat, L. G., Abelson, J., & Millert, J. H. (1986). Construction of two Escherichia coli amber suppressor genes: tRNAPheCUA and tRNACysCUA. *Proceedings of the American Thoracic Society*, *83*(September), 6548–6552.

Oda, M., Morita, M., Unno, H., & Tanji, Y. (2004). Rapid detection of *Escherichia coli* O157 : H7 by using green fluorescent protein-labeled PP01 bacteriophage. *Applied and Environmental Microbiology*, *70*(1), 527–534.

Olsen, E. V, Sorokulova, I. B., Petrenko, V. a, Chen, I.-H., Barbaree, J. M., & Vodyanoy, V. J. (2006). Affinity-selected filamentous bacteriophage as a probe for acoustic wave biodetectors of Salmonella typhimurium. *Biosensors & Bioelectronics*, *21*(8), 1434–1442.

Pavoni, E., Vaccaro, P., Pucci, A., Monteriù, G., Beghetto, E., Barca, S., De Placido, S., Martignetti, A., Felici, F., Cortese, R., & Minenkova, O. (2004). Identification of a panel of tumor-associated antigens from breast carcinoma cell lines, solid tumors and testis cDNA libraries displayed on lambda phage. *BMC Cancer*, *4*, 78.

Petrenko, V. a., & Vodyanoy, V. J. (2003). Phage display for detection of biological threat agents. *Journal of Microbiological Methods*, *53*(2), 253–262.

Petty, N. K., Evans, T. J., Fineran, P. C., & Salmond, G. P. C. (2007). Biotechnological exploitation of bacteriophage research. *Trends in Biotechnology*, *25*(1), 7–15.

Piersanti, S., Cherubini, G., Martina, Y., Salone, B., Avitabile, D., Grosso, F., Cundari, E., Di Zenzo, G., & Saggio, I. (2004). Mammalian cell transduction and internalization properties of lambda phages displaying the full-length adenoviral penton base or its central domain. *Journal of Molecular Medicine (Berlin, Germany)*, *82*(7), 467–476.

Ptashne, M. (2004). *A Genetic Switch - Phage Lambda Revisited*. (A. Gann, J. Inglis, M. Frey, & S. Schaefer, Eds.) (Third Edit., pp. 1–147). Cold Springs Harbor, New York: John Inglis.

R Development Core Team. R: A language and environment for statistical computing. (2011). *R: A language and environment for statistical computing.* Retrieved from http://www.r-project.org

Remaut, E., Stanssens, P., & Fiers, W. (1981). Plasmid vectors for high-efficiency expression controlled by the pL promoter of coliphage lambda. *Gene*, *15*, 81–93.

Ren, Z. J., Lewis, G. K., Wingfield, P. T., Locke, E. G., Steven, A. C., & Black, L. W. (1996). Phage display of intact domains at high copy number : A system based on SOC , the small outer capsid protein of bacteriophage T4. *Protein Science, 5*, 1833–1843.

Rinas, U., & Hoffmann, F. (2004). Selective leakage of host-cell proteins during high-cell-density cultivation of recombinant and non-recombinant *Escherichia coli*. *Biotechnology Progress, 20*(3), 679–687.

Roberts, J. W., & Devoret, R. (1983). Lysogenic Induction. In R. W. Hendrix, J. W. Roberts, F. W. Stahl, & R. A. Weisberg (Eds.), *Lambda II* (pp. 123–144). Cold Springs Harbor, New York: Cold Spring Harbor Laboratory.

Roberts, J. W., Roberts, C. W., & Craig, N. L. (1978). *Escherichia coli recA* gene product inactivates phage X repressor. *Sciences-New York, 75*(10), 4714–4718.

Saïda, F., Uzan, M., Odaert, B., & Bontems, F. (2006). Expression of highly toxic genes in *E. coli:* special strategies and genetic tools. *Current Protein and Peptide Science*, *7*(1), 47–56.

Santini, C., Brennan, D., Mennuni, C., Hoess, R. H., Nicosia, A., Cortese, R., & Luzzago, A. (1998). Efficient display of an HCV cDNA expression library as C-terminal fusion to the capsid protein D of bacteriophage lambda. *Journal of Molecular Biology*, *282*(1), 125–135.

Sapinoro, R., Volcy, K., Rodrigo, W. W. S. I., Schlesinger, J. J., & Dewhurst, S. (2008). Fc receptor-mediated , antibody-dependent enhancement of bacteriophage lambda-mediated gene transfer in mammalian cells. *Virology*, *373*, 274–286.

Seow, Y., & Wood, M. J. (2009). Biological gene delivery vehicles: beyond viral vectors. *Molecular Therapy : The Journal of the American Society of Gene Therapy*, *17*(5), 767–777.

Sheldon, K. A. (2013). *Two Dimensional Genetic Approach to the Development of a Controllable Lytic Phage Display System*. University of Waterloo.

Smith, G. P. (1985). Filamentous Fusion Phage : Novel Expression Vectors that Display Cloned Antigens on the Virion. *Advancement Of Science*, *228*(4705), 1315–1317.

Smith, H. E. (2007). The transcriptional response of *Escherichia coli* to recombinant protein insolubility. *Journal of Structural and Functional Genomics*, *8*(1), 27–35.

Smith, H., & Huggins, M. (1982). Successful treatment of experimental *Escherchia coli* infections in mice using phage : its general superiority over antibiotics. *Journal of General Microbiology*, *128*, 307–318.

Sokolenko, S., Nicastro, J., Slavcev, R., & Aucoin, M. G. (2012). Graphical analysis of flow cytometer data for characterizing controlled fluorescent protein display on lambda phage. *Cytometry. Part A : The Journal of the International Society for Analytical Cytology*, *81*, (12), 1031–1039.

Sorokulova, I. B., Olsen, E. V, Chen, I.-H., Fiebor, B., Barbaree, J. M., Vodyanoy, V. J., Chin, B., & Petrenko, V. A. (2005). Landscape phage probes for *Salmonella typhimurium. Journal of Microbiological Methods*, *63*(1), 55–72.

Sperinde, J. J., Choi, S. J., & Szoka, F. C. (2001). Phage display selection of a peptide DNase II inhibitor that enhances gene delivery. *The Journal of Gene Medicine*, *3*(2), 101–108.

Sternberg, N., Hamilton, D., Weisberg, R., & Enquist, L. (1979). A Simple technique for the isolation of deletion mutants of phage lambda. *Cancer Research*, *8*, 35–51.

Sternberg, N., & Hoess, R. H. (1995). Display of peptides and proteins on the surface of bacteriophage lambda. *Proceedings of the National Academy of Sciences of the United States of America*, *92*(5), 1609–1613.

Sussman, R., & Jacob, F. (1962). Sur un systeme de repression thermosensible chez le bacteriophage d'*Escherichia coli. Comptes Rendus Hebdomadaires Des Séances de l'Académie Des Sciences*, (254), 1517–1519.

Szybalski, W., Bovre, K., Fiandt, M., Guha, a, Hradecna, Z., Kumar, S., Lozeron, H.A., Maher, V.M., Nijkamp, H.J., Summers, W.C., & Taylor, K. (1969). Transcriptional controls in developing bacteriophages. *Journal of Cellular Physiology*, *74*(2), Suppl 1:33–70.

Taira, H., Matsushita, Y., Kojima, K., & Hohsaka, T. (2006). Development of amber suppressor tRNAs appropriate for incorporation of nonnatural amino acids. *Nucleic Acids Symposium Series (2006)*, *50*, 233–4.

Tanji, Y., Shimada, T., Yoichi, M., Miyanaga, K., Hori, K., & Unno, H. (2004). Toward rational control of Escherichia coli O157:H7 by a phage cocktail. *Applied Microbiology and Biotechnology*, *64*(2), 270–274.

Tao, P., Mahalingam, M., Marasa, B. S., Zhang, Z., Chopra, A. K., & Rao, V. B. (2013). In vitro and in vivo delivery of genes and proteins using the bacteriophage T4 DNA packaging machine. *Proceedings of the National Academy of Sciences of the United States of America*, *110*(13), 4–9.

Thomas, B. S., Nishikawa, S., Ito, K., Chopra, P., Sharma, N., Evans, D. H., Tyrrell, D., Lorne, J., Bathe, Oliver F Rancourt, D. E. (2012). Peptide vaccination is superior to genetic vaccination using a recombineered bacteriophage subunit vaccine. *Vaccine*, *30*(6), 998–1008.

Turnbough, C. L. (2003). Discovery of phage display peptide ligands for species-specific detection of *Bacillus* spores. *Journal of Microbiological Methods*, *53*(2), 263–271.

Vaccaro, P., Pavoni, E., Monteriù, G., Andrea, P., Felici, F., & Minenkova, O. (2006). Efficient display of scFv antibodies on bacteriophage lambda. *Journal of Immunological Methods*, *310*(1-2), 149–158.

Valdez-Cruz, N. A, Caspeta, L., Pérez, N. O., Ramírez, O. T., & Trujillo-Roldán, M. A. (2010). Production of recombinant proteins in *E. coli* by the heat inducible expression system based on the phage lambda pL and/or pR promoters. *Microbial Cell Factories*, *9*, 18.

Vallejo, L. F., Brokelmann, M., Marten, S., Trappe, S., Cabrera-Crespo, J., Hoffmann, A., Gross, G., Weich, H. A., & Rinas, U. (2002). Renaturation and purification of bone morphogenetic protein-2 produced as inclusion bodies in high-cell-density cultures of recombinant *Escherichia coli. Journal of Biotechnology*, *94*(2), 185–194.

Villaverde, A., Benito, A., Viaplana, E., & Cubarsi, R. (1993). Fine regulation of c1857-controlled gene expression in continuous culture if recombinant *Escherichia coli* by temperature. *Applied and Environmental Microbiology*, *59*(10), 3485–3487.

Wegrzyn, G., & Wegrzyn, A. (2002). Stress responses and replication of plasmids in bacterial cells. *Microbial Cell Factories*, *1*(1), 2.

Wendt, J. L., & Feiss, M. (2004). A fragile lattice: replacing bacteriophage lambda's head stability gene D with the shp gene of phage 21 generates the Mg2+-dependent virus, lambda shp. *Virology*, *326*(1), 41–46.

Westwater, C., Kasman, L. M., Schofield, D. A., Werner, P. A., Dolan, J. W., Schmidt, M. G., & Norris, J. S. (2003). Use of genetically engineered phage to deliver antimicrobial agents to bacteria: an alternative therapy for treatment of bacterial infections. *Antimicrobial Agents and Chemotherapy*, *47*(4), 1301–1307.

Wickham, H. (2009). ggplot2: elegant graphics for data analysis.

Willats, W. G. T. (2002). Phage display: practicalities and prospects. *Plant Molecular Biology*, *50*, 837–854.

Windass, J. D., & Brammar, W. J. (1979). Aberrant immunity behaviour of hybrid of ColE1-type plasmids phages containing the DNA, *172*, 329–337.

Witkiewiczl, H., & Schweiger, M. (1982). The head protein D of bacterial virus chromosomal proteins. *EMBO Journal*, *1*(12), 1559–1564.

Yamamori, T., & Yura, T. (1980). Temperature-induced synthesis of specific proteins in *Escherichia coli*: evidence for transcriptional control. *Journal of Bacteriology*, *142*(3), 843–851.

Yang, F., Forrer, P., Dauter, Z., Conway, J. F., Cheng, N., Cerritelli, M. E., Steven, A. C., Plückthun, A., & Wlodawer, A. (2000). Novel fold and capsid-binding properties of the lambda-phage display platform protein gpD. *Nature Structural Biology*, *7*(3), 230–237.

Zakharova, M. Y., Kozyr, A. V, Ignatova, A. N., Vinnikov, I. A., Shemyakin, I. G., & Kolesnikov, A. V. (2005). Purification of filamentous bacteriophage for phage display using size-exclusion chromatography. *BioTechniques*, *38*(2), 2–4.

Zanghi, C. N., Lankes, H. a, Bradel-Tretheway, B., Wegman, J., & Dewhurst, S. (2005). A simple method for displaying recalcitrant proteins on the surface of bacteriophage lambda. *Nucleic Acids Research*, *33*(18), e160.

Zanghi, C. N., Sapinoro, R., Bradel-Tretheway, B., & Dewhurst, S. (2007). A tractable method for simultaneous modifications to the head and tail of bacteriophage lambda and its application to enhancing phage-mediated gene delivery. *Nucleic Acids Research*, *35*(8), e59.

Zhao, K., Liu, M., & Burgess, R. R. (2005). The global transcriptional response of *Escherichia coli* to induced sigma 32 protein involves sigma 32 regulon activation followed by inactivation and degradation of sigma 32 in vivo. *The Journal of Biological Chemistry*, *280*(18), 17758–17768.

Zucconi, a, Dente, L., Santonico, E., Castagnoli, L., & Cesareni, G. (2001). Selection of ligands by panning of domain libraries displayed on phage lambda reveals new potential partners of synaptojanin 1. *Journal of Molecular Biology*, *307*(5), 1329–1339.

Copyright Acknowledgements

This work was funded by the Canadian Institute for Health Research (DSECT) trainee program to JN and, Human Resources and Skill Development Canada (HRSDC) and Natural Sciences and Engineering Research Council of Canada (NSERC) funding to RAS